IMPACT OF STRAND GEOMETRY AND ORIENTATION ON MECHANICAL PROPERTIES OF STRAND COMPOSITES

By

KRISTIN LYNNE MEYERS

A thesis submitted in partial fulfillment of
the requirements for the degree of

MASTER OF SCIENCE IN CIVIL ENGINEERING

WASHINGTON STATE UNIVERSITY
Department of Civil and Environmental Engineering

December 2001

To the Faculty of Washington State University:

The members of the Committee appointed to examine the thesis of KRISTIN LYNNE MEYERS find it satisfactory and recommend that it be accepted.

_____
Chair

_____

_____

ACKNOWLEDGEMENT

The author appreciates, most of all, her advisor, Dr. Michael Wolcott. His unending patience and encouragement combined with a vast knowledge and skill at guiding without dictating made the authors graduate experience priceless. The author would also like to thank Dr. John Hermanson, a committee member, for his help with evaluating the non-linear E, material mechanics explanations and, of course, Mathematica tutoring. Dr. David Pollock, the final committee member, kept engineering and applications in the author's mind and kept her sanity intact with an unfailing positive outlook.

The author would also like to thank all of her fellow graduate students. She would like to thank Vikram Yadama for his partnership in strand and panel production and for his endless supply of information and technical literature. She also wants to thank Karl Englund and David Harper for all of the time they volunteered in their respective areas of expertise and for all of the high fat, low nutritional and intellectual value lunches. Pete Cates is also appreciated for all of the time spent in the manufacturing of the panels. Oh yeah, and that crazy Bill Parsons, who made her welcome when she first started and later provided entertainment for the before mentioned lunches with Karl and David.

The staff of the WMEL were also invaluable. Bob Duncan helped, not only to teach the author to operate the hot presses, but gave the author practical lab knowledge. Marty Lentz came out of retirement for three months to help in the panel manufacture. Scott Lewis created the LVDT holders used in all tension test and helped with many small tasks. Finally, Dave Dostal, with his infinite patience, helped with test set-ups that always seemed simple, but never were, taught the author to write data acquisition programs and always has a practical and simple solution to any problem.

The author would also like to thank Chris Brandt for all of his support and his help with taking the digital images of all the panels. Without the pressure from Chris and Bill she would not be on her way to Boise. She would also like to thank her parents and sister for all of the encouragement and love. Finally, she would like to thank her grandfather for always believing she would succeed and for never letting her wonder if she was cared for.

IMPACT OF STRAND GEOMETRY AND ORIENTATION

ON MECHANICAL PROPERTIES OF

STRAND COMPOSITES

Abstract

By Kristin Lynne Meyers, M.S.
Washington State University
December 2001

Chair: Michael P. Wolcott

Structural strand composite literature often cites strand geometry as a factor controlling mechanical properties. This effect is quantified through empirically relating the strand slenderness ratio, the ratio of strand length to thickness, to composite properties. The research presented here examines the effect of strand length and width separately by maintaining a single nominal thickness for three nominal strand lengths and widths, 10, 20 and 30 cm and 1.25, 1.9 and 2.5 cm respectively. In addition, the effect of strand orientation in the panel was considered apart from strand geometry by forming each geometry at two orientation levels. Tensile and compressive properties were assessed for both the parallel and transverse directions of each panel. Statistical analysis indicated that parallel tensile and compressive elastic modulus (E) and strength (σ_{ult}) do not rely on strand length or width within the range tested. Strand length is only significant by influencing orientation. Panel properties were influenced primarily by strand orientation and density, thus the need for long strands is only to attain adequate orientation.

In addition, multiple predictive models were evaluated. Fully or semi-empirical models are generally used in the literature to predict properties, limiting these models to the scope of the original test data. A mechanics of materials approach, considered in this research, would not have these same limitations. Test data was compared with predicted values from a model

developed by Barnes (2000), the Hankinson equation and tensor transformation, using either the mean angle or a distribution of angles and the rule of mixtures (ROM). Tensor transformation with the ROM, a mechanics of materials approach, predicted parallel properties consistently well, while Barnes' model, a semi-empirical method, was accurate using a measured mean angle to predict parallel properties, but did not consistently predict values within the same percent error range. Hankinson's equation using a recommended exponent of 2, did not work well with a mean strand angle or the ROM.

TABLE OF CONTENTS

LIST OF TABLES

LIST OF FIGURES

CHAPTER 1

INTRODUCTION

ABSTRACT

Many factors that influence oriented strand composite properties have been identified in the literature. Two of the prominent factors are strand geometry and in-plane orientation. The following research assesses the statistical and practical importance of these individual factors to identify influential factors and apply these factors to a model. Strand composite literature is reviewed with emphasis on effects of and models for strand geometry and orientation. This chapter presents a review of the relevant research, the second chapter presents a database and identifies significant factors and trends, the third chapter presents and compares models and the fourth chapter discusses the conclusions drawn from this research.

INTRODUCTION

Composite lumber products extend raw material yield and facilitate utilization of smaller diameter trees (McNatt 1990). One such product that replaces solid sawn structural components is oriented strand lumber (OSL). Increased consistency and densities of these products often elevate the 5^{th} percentile design properties to levels above those of solid lumber used in the composite (Knudson 1992). These properties make OSL a highly competitive engineered alternative to traditional lumber.

Oriented strand board (OSB) is a panel product that also utilizes shorter strands, 10 cm as compared to 30 cm for OSL. OSB is primarily used in panel applications, such as sheathing, while OSL was developed for use as structural members including beams and columns. The

differences between these products are the often layered alignment and lower mechanical properties of OSB.

Development of OSL was largely a result of empirical experiments and manufacturing experience (Triche & Hunt 1993), leaving much of the knowledge proprietary. Statistical models for strand composites have been developed using specific experimental data with some success, however, the models are generally too narrow to be widely used.

OSB strands are easily handled in production environments, while OSL strands are susceptible to curl and breaking, creating forming difficulties. Despite the difference in strand geometry, single layer OSB can achieve properties at OSL levels. Shupe *et. al*. (2001) measured an OSL level bending MOE of 12404 MPa with strands 7.6 cm in length. The ability to use shorter strands to obtain OSL level properties would improve many components of manufacturing facilitating conversion of OSB plants to the commercially expensive OSL. To assess this possibility, the factors that influence properties in strand composites have to be separated, tested and significance identified. A design procedure based on mechanics of materials would allow application beyond the scope of empirical equations fit to data with a finite range.

The following research evaluates fundamental and empirical models for strand composites. Panels were manufactured with known strand lengths, widths and orientation. Each panel type, was evaluated in tension and compression both parallel and transverse to the axis of the preferred alignment. Young's modulus, E, and strength were determined by each test. These properties were used as response variables in analyses of variance (ANOVA) and the factors that have a significant effect were addressed in modeling.

OBJECTIVES

Factors influencing the mechanical properties of oriented strand composites have not been effectively evaluated. This research identifies factors influential to panel properties and evaluates design procedures to aid in the understanding of the parameters able to modify properties and help in the predictive capabilities of the literature.

1. Assess parallel and transverse tensile and compressive properties of aspen OSL produced with multiple strand geometries and orientations.
2. Examine trends illustrated by data and identify factors that significantly influence board properties in order to evaluate the need for long strand lengths.
3. Appraise validity and compare effectiveness of two-dimensional semi-empirical and fundamental material design procedures.

LITERATURE REVIEW

The majority of current models used to design or predict wood-strand composite properties are empirical. Possible inputs for these models are vast. Thus, to obtain a practical design procedure a researcher must focus on the factors that are the most influential. Two such components are strand geometry and in-plane orientation. Much of the research currently in the literature have, in many cases, failed to separate interacting variables, including strand geometry and orientation.

Geometry

Nelson (1997) cites strand geometry as crucial in obtaining optimum board properties. The slenderness ratio (L/d where L is the strand length and d is the strand thickness) has often been used to develop empirical equations specific to each research project. However, much of

the research that studies slenderness ratio did not separate the effect of orientation. Post (1958) and Suchsland (1968) both found that the modulus of rupture of flakeboard increases with increasing slenderness ratio. MOR properties asymptotically approached a constant value at high slenderness ratios, the ratio of strand length to thickness. Wang and Lam (1999) developed empirical relationships for MOR and MOE using slenderness ratio, surface orientation and panel density. For flake lengths from 5.0 to 10 cm and a thickness of 0.06 cm the optimum slenderness ratio was identified as 133, or a strand of approximately 8.0 cm.

Hoover *et al*. (1992) developed empirical regression models relating various properties to flake length and thickness, board density, an alignment factor found using stress-wave timing. All factors were experimentally determined and included in the model, significant or not, to account for the maximum variation. The model for parallel tensile modulus described the property for the 5.0 to 7.6 cm long strands, to within 18% of actual values with a COV of 56.2%. However, No practical difference existed in properties for the strand geometries evaluated. Lehmann (1974) developed a model with similar variables and achieved an r^2 value of 0.878. However, model versatility was limited by short flake lengths of 1.25, 2.5 and 5.0 cm and by omitting strand orientation. General trends were discussed and specific equations were developed with limited applicability.

Finite Element Model

Triche and Hunt (1993) developed a finite element (FE) based model to predict tensile properties of oriented strand board (OSB). Extensive nondestructive testing was used to characterize the size and stiffness of strands. This data was then used to divide the strands into stiffness (E) classes including random (strands of random stiffness), extreme (strands of high and low stiffness), low, high and medium. Each strand and the corresponding resin interface was

represented in the FE program as a single “superelement”, which was generated using a Fortran program by combining adjacent 8-noded rectangular elements. If this process was used to model an entire OSB panel, the element structure would be repeated, limiting variability. Model validity was assessed by comparing hand laid strand assemblies with individual strands within a single property class with simulated panel properties. The model had a maximum error of 101.1%, for boards made using the medium stiffness class and a minimum error for the low class of 1.2%.

In Plane Orientation Model

In plane orientation is a major factor affecting composite properties. It is measured for OSL as the angle between a strand and the preferred axis of the panel. Mean angle is calculated by measuring multiple angles, finding the average of the absolute values of the measured angles. The mean is then used to describe orientation within a panel. Values of E and strength in the parallel board direction increase with higher levels of orientation. The first 20 degrees of off-axis alignment can reduce properties to near half of solid-sawn properties (Wood Handbook 1987). This drop is not linear and is generally modeled empirically.

The Hankinson equation (Equation 1.1) is an empirical formula used to transform parallel (E_1) and transverse (E_2) stiffness property values to those of some arbitrary angle (E_θ). As the mean angle of orientation, θ, decreases E_θ approaches E_1. Use of the Hankinson equation with a mean angle is the most common way to reduce parallel aligned properties to properties of with off-axis orientation (Wood Handbook 1987, Barnes 2000).

$$E_\theta = \frac{E_1 E_2}{E_1 \sin^n \theta + E_2 \cos^n \theta} \qquad \text{Equation 1.1}$$

Where n = is an empirical factor used to fit data to the Hankinson equation, for modulus of elasticity n=2 if E_2/E_1 = 0.04 to 0.12 (Wood Handbook)

Xu and Suchsland (1998) developed a volume-based rule of mixtures (ROM) for composite E that incorporates alignment and strand volume by equating the elastic energy and work (Equation 1.2). The (ROM) is a weighted average that, in combination with the Hankinson equation, accounts for orientation effects. This method allows a distributional approach to the Hankinson equation.

$$E = \sum \frac{V_i E_\theta}{V} \qquad \text{Equation 1.2}$$

Where: V_i is the volume fraction of the i^{th} group, oriented in the θ direction. V is the total volume fraction.

Simpson (1977) used the rule of mixtures to predict tensile strength of OSB from the strand tensile strength and the shear strength of the adhesive. The fraction of flakes failing in tension multiplied by the tensile strength was added to the product of the fraction of adhesive pull out failures and shear strength. Further, the ratio of pull out to tensile failures is assumed proportional to the ratio of the force to fail the flake to the force to pull the flake out. After manipulating the forces and geometry terms the tensile strength is found to be a function of strand geometry as seen in Equation 1.3 (Simpson 1977).

$$T_b = \frac{T_w(r+k)}{r+ku} \qquad \text{Equation 1.3}$$

Where: T_w = tensile strength of flake, r = l/t l= strand length, t = strand thickness, k = proportionality constant (assumed equal to 1), u = T_w/S and S = shear strength of adhesive bond

Geometry Models

The stress transfer angle is used to describe the effect of strand length mechanically (Barnes 2001). This is accomplished by attributing increasing parallel properties with longer strands to the decreasing angle at which stress is transferred between strands. The stress transfer angle relies on strand length and thickness.

For the assumed assembly, the glue-line is assumed equal to half the strand length. For an entire composite panel, failure will occur at the shortest average glue-line length for any cross section in the board. The mean glue line is also assumed half the strand length. Equation 1.4 defines ϕ (Barnes 2001).

$$\phi = \arctan\left(2d_b / L\right) \qquad \text{Equation 1.4}$$

Where, L is the mean strand length, d_b is the mean in situ strand thickness and is equal to $d_a(a/b)$ where, a = initial dry wood density, b = dry density of product, d_a = average initial strand thickness

The stress transfer angle is assumed to affect properties similar to in-plane angles and therefore the Hankinson equation (Equation 1.1) is used to predict E_ϕ. For infinitely long strands, ϕ is very small and E_ϕ approaches E_1. For short strands ϕ increases and E_ϕ is closer to E_2. The Hankinson equation uses n and Barnes defines *n* for stress transfer angle as 1.5 for parallel aligned Douglas-fir flakes with a thickness of 0.1 inches. In contrast, *n* = 1.0 was needed for thinner (0.02<t<0.04 in.) aspen strands in a multi-layer product. In both cases, these exponents are less than the recommended n = 2.0 (Wood Handbook 1987).

The Halpin-Tsai equations are a semi-empirical method that is traditionally used for short fiber composites embedded in a matrix. These equations are generally applied for fiber volume

fractions less than 0.7. The Halpin-Tsai equations were developed from the rule of mixtures by adding an empirical factor to account for discontinuities in short fiber composites (Halpin 1969).

Prediction of E_1 and E_2 of a composite material produced with oriented discontinuous fiber elements is possible using the Halpin-Tsai equations. E_c is the composite E for both directions found using Equation 1.5 (Halpin 1984).

$$E_c = E_m\left(\frac{1+\xi\eta v_f}{1-\eta v_f}\right) \qquad \text{Equation 1.5}$$

$$\eta = \frac{E_f/E_m - 1}{E_f/E_m + \xi} \qquad \text{Equation 1.6}$$

Where, v_f is the volume fraction of the fiber, E_m is the E of the matrix, E_f is the E of the fiber and η is defined by Equation 1.6

In applying this approach to cellular wood-based composites, Shaler and Blankenhorn (1990) took E_f as the E of the cell wall material without air voids. ξ is an empirical factor intended to quantify the amount of load transmitted from the fiber to the matrix and is often a function of the fiber slenderness ratio (L/d). Shaler and Blankenhorn (1990) defined ξ equal to $2(l/d)$ for the parallel panel direction and assume that strand geometry does not affect the transverse direction by applying $\xi = 2$. Halpin (1984) defines ξ for "oriented discontinuous ribbon or lamella-shaped reinforcement" for the parallel direction as Equation 1.7.

$$\xi = 2(L/t) + 40v_f^{10} \qquad \text{Equation 1.7}$$

Where, ξ for the transverse direction is redefined by substituting (w/t) for (L/t) in equation 1.7 (Halpin 1984). The Halpin-Tsai equations have traditionally been used for small volume fractions of fiber, allowing the far right term to be neglected (Chawla 1987).

SUMMARY

The literature has an abundance of research completed analyzing the effect of strand geometry and of in-plane strand orientation on panel properties. Much of this research cites strand geometry as significant, but is based on strands that are much shorter than those used for OSL. In addition, a void exists in the separation of geometry and orientation. The following chapters explain how the factors were divided into distinct variables. For this research, analyses of variance were then used to determine significance. Density and orientation were significant for parallel tensile and compressive E, illustrating the independence of E from strand geometry over the observed lengths and widths. Two orientation models, the Hankinson equation and tensor transformation, were applied using both mean angles and the normal and 2-parameter Weibull distributions with some success. Also evaluated, is a semi-empirical model introduced by Barnes (2000), which predicted properties accurately. The ability to utilize shorter, easier to handle strands in composites with intended structural member uses does exist. However, higher levels of orientation will have to be achieved.

REFERENCES

Barnes, Derek. *An Integrated Model of the Effect of Processing Parameters on the Strength Properties of Oriented Strand Wood Composites*. Forest Products Journal. 50(11/12), 2000. pp. 33-42.

Barnes, Derek. *A Model of the Effect of Strand Length and Strand Thickness on the Strength Properties of Oriented Wood Composites.* Forest Products Journal. 51(2), 2001. pp. 36-46.

Chawala, K.K.. *Composite Materials: Science and Engineering.* Springer-Verlag New York, Inc., New York. 1987. pp. 184-186.

Halpin, J.C. *Stiffness and Expansion Estimates for Oriented Short Fiber Composites.* Journal of Composite Materials. 3, 1969. pp. 732-735.

Halpin, J.C.. *Primer on Composite Materials: Analysis*. Technomic publishing Co. Inc., Lancaster, Pennsylvania. 1984. pp. 130-142.

Hoover, William L., Michael O. Hunt, Robert C. Lattanzi, James H. Bateman, John A. Youngquist. *Modeling Mechanical Properties of Single-Layer, Aligned, Mixed-Hardwood Strand Panels*. Forest Products Journal. 42(5). 1992. pp. 12-18.

Knudson, R.M. *PSL 300^{TM} LSL: The Challenge of a New Product*. Proceedings of the Twenty-Sixth Washington State University International Particleboard/Composite Materials Symposium. 1992. Pp. 206-214.

Lehmann, W.F. *Properties of Structural Particleboards*. Forest Products Journal. January 1974 24(1). pp. 19-26.

McNatt, J. Dobbin, and Moody, Russell C. Structural Composite Lumber. Progressive Architecture. pp 34-36. December 1990.

Nelson, Sherman. Engineered Wood Products; A Guide for Specifiers, Designers and Users: Chapter 6 - Structural Composite Lumber. pp 6-147 to 6-172. 1997 PFS Research Foundation. Madison, WI.

Post, P.W. *Effect of Particle Geometry and Resin Content on Bending Strength of Oak Flake Board*. Forest Products Journal. October 1958. pp. 317-322.

Shaler, Stephen M. and Paul R. Blankenhorn. *Composite Model Prediction of Elastic Moduli for Flakeboard.* Wood and Fiber Science. 22(3), 1990. pp. 246-261.

Shupe, T.F., C.Y. Hse and E.W. Price. *Flake Orientation Effects on Physical and Mechanical Properties of Sweetgum Flakeboard*. Forest Products Journal. 51(9), 2001. pp. 38-43.

Simpson, William T. *Model for Tensile Strength of Oriented Flakeboard*. Wood Science. 10(2), October 1977. pp.68-71.

Suchsland, Otto. *Particle-Board From Southern Pine*. Southern Lumberman. December 1968. pp. 139-144.

Triche, Michael H., and Hunt, Michael O. *Modeling of Parallel-Aligned Wood Strand Composites*. Forest Products Journal. Vol. 43 #11/12 1993. pp. 33-44.

Wang, Kaiyuan and Lam, Frank . *Quadratic RSM Models of Processing Parameters for Three-layer Oriented Flakeboard*. Wood and Fiber Science. April 1999, 31(2). pp. 173-186.

Wood Handbook #72 1987.U.S. Forest Products Laboratory, pp 4-14, 4-25, 4-29.

Xu, Wei and Suchsland, Otto. *Modulus of Elasticity of Wood Composite Panels with a Uniform Vertical Density Profile: A Model*. Wood and Fiber Science. 30(3), 1998. pp. 293-300.

CHAPTER 2

THE EVALUATION OF THE RELIANCE OF STRUCTURAL STRAND COMPOSITES ON STRAND GEOMETRY

ABSTRACT

The reliance of structural strand composite properties on strand geometry has been the subject of much research. Commercial strand products currently use strands in the range of 10-30 cm to service different structural demands. However, the correlation between strand length and improved material properties has not been conclusively established. The research presented in this paper first establishes a database of material properties for single layer oriented strand composites. Panels were produced with multiple strand lengths and widths, while varying the level of orientation, separating the effect of strand geometry orientation. Tensile and compressive properties were assessed for both the parallel and transverse directions of each panel. The parallel elastic modulus (E) and strength (σ_{ult}) for both tension and compression did not statistically rely on strand length or width when strand orientation was included in the statistical model. However, strand length significantly impacts strand orientation when using mechanical strand alignment. Tensile parallel properties are consistently higher than the values obtained for parallel compression, while the transverse properties for compression and tension are similar. Interpretation of the data obtained in this study indicates that there is no need for longer strand lengths to achieve adequate OSL properties if adequate orientation is achieved with the shorter strands. The role of adequate strand orientation appears to have much greater importance than strand geometry.

INTRODUCTION

Composite lumber products extend the yield for and improve the utilization of smaller diameter trees. One such product with the potential for replacing solid sawn structural components is oriented strand lumber (OSL). Increased consistency and densities often elevates the 5th percentile design properties for OSL to levels above those of solid lumber used in the composite (Knudson 1992). These properties make OSL a highly competitive engineered alternative to traditional lumber.

To date, the development of OSL is largely a result of empirical experiments and manufacturing experience (Triche & Hunt 1993), leaving much of the knowledge proprietary. Statistical models for OSL have been developed using specific experimental data with some success; however, the models are generally too narrow to be widely applicable.

Nelson (1997) cites strand geometry as crucial in obtaining optimum board properties. The slenderness ratio (ratio of strand length to thickness; L/d) has often been used to develop empirical equations and identification of property trends specific to each research project (Post 1958, Brumbaugh 1960, Suchsland 1968). However, much of the research that studies slenderness ratio does not explicitly separate the effect of strand orientation from geometry. Two such projects are Post (1958) and Suchsland (1968) who found that the modulus of rupture of flakeboard increases with increasing slenderness ratio. However, MOR properties asymptotically approached a constant value at high slenderness ratios. In addition, Wang and Lam (1999) developed empirical relationships for MOR and MOE with slenderness ratio, surface orientation and panel density using three-dimensional surface maps to generate quadratic regression models for a multi-layer strand composite with oriented faces and a random core. Mats were robotically formed to ensure each face strand was aligned at an angle defined by the

normal distribution. The resulting equations used a single angle to describe orientation. For flake lengths from 5 to 10 cm and a thickness of 0.6 mm the optimum slenderness ratio was identified as 133, or a strand of approximately 8 cm. Barnes (2000) found that increasing strand length increased the modulus of elasticity (MOE) along the parallel axis of the panel and modulus of rupture (MOR) for strands 7.5 to 30 cm long.

Hoover *et al*. (1992) developed empirical regression models relating various properties to flake length and thickness, board density, an alignment factor found using stress-wave timing and an error term. All factors were experimentally determined and included, significant or not, in the model to account for the maximum variation. The model for parallel tensile modulus described the property for the 5.0 to 7.6 cm long strands, to within 18% of actual values with a COV of 56.2%. Although length significantly affected panel properties and was included in the model, the author noted that no practical difference existed in properties for the strand geometries evaluated.

Lehmann (1974) developed another model with similar variables. An r^2 value of 0.878 was achieved, however model versatility was limited because shorter flake lengths were used. In this study, strands with lengths of only 1.25, 2.5 and 5.0 cm were included and the influence of strand orientation was not separated from length effects. General trends are discussed and specific equations are developed with limited applicability. The studies have, in many cases, failed to separate two variables that are tightly bound, such as geometry and orientation.

OBJECTIVES

The ability to achieve properties that are characteristic of OSL with OSB length strands would allow the OSL industry to grow with minimal capital investment by converting existing

production facilities to the different product line. Toward this goal, the specific objectives of this research are to:

1. Assess within-plane tensile and compressive properties of aspen oriented strand lumber (OSL) produced with multiple strand geometries and orientation levels.
2. Identify material design factors that significantly impact these properties.
3. Assess the strand geometry needed to attain specific properties.

METHODS AND MATERIALS

Strand Preparation

Aspen (*Populus tremuloides* Michx.*)* trees were harvested from a stand on the University of Idaho Experimental Forest, near Moscow, Idaho. Logs were sawn into boards with thicknesses corresponding to the target strand widths using a portable band mill. Strands were then cut from the edges of these boards using a laboratory-scale ring strander (CAE 12/48). The strands were screened and dried to a moisture content of approximately 3%, eliminating fines, the all strands passed a 4.5 cm screen.

Panel Manufacture

Single layer, oriented panels were hot pressed at 182°C using 6% liquid PF resin solids (GP® 130C44 RESI-STRAN®) to a target thickness and density of 1.9 cm and 593 kg/m^3; respectively. The 15-minute press-schedule included 30 seconds close time, 810 second hold and 60 second vent and was developed using a temperature and gas probe. Panels were manufactured for multiple strand geometries and levels of orientation. Three nominal strand

lengths (10, 20 and 30 cm) and widths (1.25, 1.9 and 2.5 cm) were used with a single thickness of 0.076 cm.

Oriented mats were hand formed using an oscillating forming box equipped with vanes spaced at 3.8 and 7.6 cm to create different degrees of orientation. Panels were formed with both vane spacings for the 10 and 20 cm strands. Panels made of the 30 cm strands were formed using only the 7.6 cm spacing because the strand length inhibited forming with only minimal improvements to alignment at the 3.8 cm spacing. For each geometry and vane spacing combination, three panels were pressed for a total of 45 boards.

Material Structure Characterization

The material design attributes of strand orientation and density were measured for each panel set to accurately describe the potential factors influencing board properties. Strand orientation for each panel face was quantified using digital image analysis. A total of 100 points were randomly generated on the image of each panel face. The angle a strand forms with the panel edge was measured for each marked strand. Eliminating repeated measures of individual strands, this process yielded approximately 170 measurements per panel. The angular distribution described by surface angles is assumed to be representative of the entire panel thickness (Harris & Johnson 1982 and Geimer 1993).

Six density scans for each panel were performed to find the vertical density profile using an x-ray density profiler. These samples were 5.0 cm square and are the same samples used for internal bond tests. The profiles were generally symmetric with an average core to face density ratio of 1.5, which did not, in general vary among panel types. A representative profile is shown in **Figure 1**.

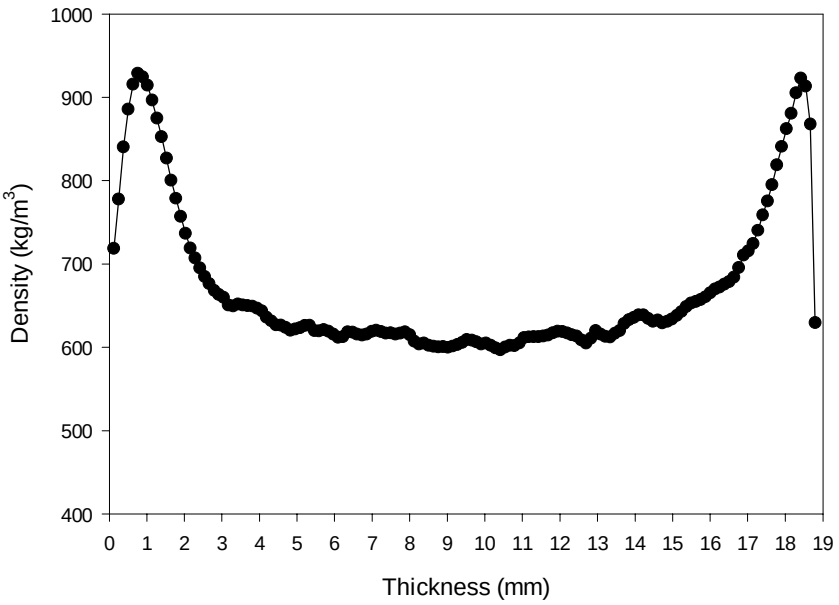

Figure 1: *Example of a typical vertical density profile*

The average moisture content of the specimens was measured to be 9.6% prior to testing in accordance with ASTM D4442-92, method B. All specimens were conditioned to 21° C and 65% relative humidity.

Mechanical Properties Characterization

Mechanical tests of the panels were conducted using either a screw driven or a servo-hydraulic universal testing machine equipped with computer data acquisition. The strain rate used for tension and compression tests was 0.01 cm/cm/min. Strain rate was used to determine cross-head movement by dividing the length of the specimen by the speed of the cross-head and equating that with the strain rate. Nine tests were performed for both tension and compression for each direction, geometry and vane spacing combination. The elastic modulus (E) and strength (σ_{ult}) both parallel and transverse to the strong axis of the panel were evaluated. Internal bond tests were performed in accordance with ASTM D1037-86a. Specimen location within a panel is defined by a single cutting pattern (Meyers 2001).

All tension tests used a one-inch stroke LVDT affixed with tabs to record specimen displacement over a specific gauge length. Testing was completed in accordance with ASTM D5456-98a and D4761-96. Specimen sizes deviate from the standard. Tension parallel specimens were 7.6 x 71 cm tapered to 5.0 cm for a gauge length of 15 cm. The specimen size is shorter than the standard specimen length, but allowed for twice the longest strand length between the grips and half the longest strand length within the gauge length. Transverse tension specimens were 7.6 x 40 cm and were also tapered to 5.0 cm for a gauge length of 7.6 cm. Strands are aligned perpendicular to this test direction, so only a single strand length was allowed for the between grips length and a quarter for the gauge length.

Compression tests were performed using a clip extensometer with a gauge length of 1 inch to measure displacement. The bottom plate of the test fixture was fixed and the top plate rotated on a ball joint. All compression specimens were tested at the same size of, 1.9 x 1.9 x 8.9 cm. The width and thickness of these specimens was less than the standard size, but was controlled by panel thickness.

Determining Elastic Modulus

Most specimens displayed a high non-linear stress-strain relationship in both tension and compression (**Figure 2**). Density variation throughout the specimen may have produced the stress-strain curves with either a concave or convex toe region at the beginning of the curve. This high degree of non-linearity posed problems for arbitrarily choosing a consistent region to define E. Attempts to utilize traditional methods were deemed subjective and not easily reproducible. Non-linear stress-strain relationships are common in many polymers and ASTM D 695-96 Standard Test Method for Compressive Properties of Rigid Plastics addresses this issue by specifying a method of determining E as the tangent to the stress-strain curve at the point of

maximum slope (1st derivative). However, the differences in curvature of the toe region evident in our data prevented the consistent use of this method. Instead, the E was determined as the tangent of the stress-strain curve at the inflection point of the slope (1st derivative), which is the local extrema of the 2nd derivative, curvature (**Figure 2**). This method was implemented by fitting a 4th order (non-linear) polynomial to the stress-strain data. The 3rd derivative of this function was then set to zero to find the extrema used to compute E. This method was easily implemented numerically and produced a reproducible point from which to calculate E in the lower stress region of the curve.

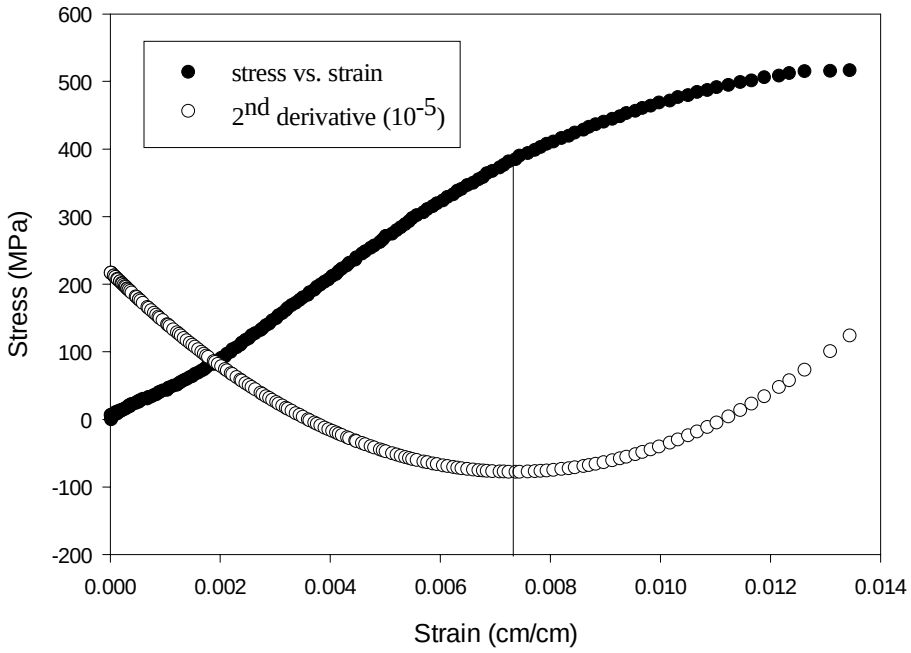

Figure 2: *Non-linear stress-strain behavior*

Statistical Methods

Multiple statistical tests were used to interpret the data. Tests identified existence of significant differences in panel properties and factors that significantly influence these properties. The most utilized analysis tool was the analysis of variance (ANOVA). All tests

were compared with a significance level of 95% with a corresponding p-value of 0.05 and were completed using SAS software unless otherwise stated.

A box-plot test was utilized to determine valid outlying data (Ostle and Malone 1988). This test defines quartiles into which the data are categorized and bases the existence of suspect and statistical outliers on the distance a data point lies from the boundaries of the 1^{st} and 3^{rd} quartiles and the spread between those boundaries.

The Kolgorov-Smirnov (K-S) 2-sample statistical test was used to find differences in the distributions of angles. This test compares the cumulative frequency distributions (CFD) of two data sets by calculating the greatest difference between the CFD's and comparing this to a test statistic, D. The null hypothesis of this test, accepted for high p-values, is that the two data sets can be described by the same distribution. In this research, this test was utilized to determine which distributions of strand orientation are statistically identical ($p>0.10$).

Differences between means were found using Tukey's test. This test accounts for experiment-wise error for experiments with unbalanced data sets. In addition, it does not require a control to which all means are compared.

RESULTS AND DISCUSSION

Mechanical Properties

Oriented strand lumber is used in applications that utilize both tensile and compressive properties. Parallel and transverse E and σ_{ult}, denoted the y-direction and x-direction respectively, were found for the panels. Both tension and compression loading were evaluated. Failures observed for compression specimens were mainly in tension perpendicular to the panel plane (**Figure 3**). This mechanism was observed along strands that had considerable curvature

and could be a result of out of plane angle that caused the strands to be loaded with eccentricity resulting in strand buckling or bending. This finding has particular note regarding panel durability especially when panels experiencing compression stresses undergo moisture changes. Linville (2000) found that a moisture content as little as 13% could result in a significant degree of panel damage from excessive tension stresses perpendicular to the panel plane. The strength reduction from this damage will decrease compressive panel strength and stiffness properties.

Figure 3: *Tension perpendicular compression failure*

Transverse tension specimens generally failed within the gauge length or in the area in which the specimen was tapered. However, nearly half of the parallel specimens experienced grip line failures. The data produced with these failures can only be interpreted as a lower limit of tension strength. Reported values for σ_{ult} were calculated based on assumed failure in the gauge length.

Mechanical properties obtained are similar to commercial strand products and solid structural use lumber (**Table 1 and Table 2**). OSB has a general average parallel MOE range of

4830 to 8270 MPa, which is lower than most of the geometry and orientation combinations. TimberStrand®, a commercial OSL produced by Trus Joist, has values of MOE from 8965 to 14480 MPa (NRCC). Douglas-fir, a common specie used as structural lumber, has an MOE of 13600 MPa (Wood Handbook). These similarities provide a reference for which the test panels can be compared to.

Length (cm)	Width (cm)	Vane Spacing (cm)	E_y (%COV) (MPa)	E_x (%COV) (MPa)	$\sigma_{ult,y}$ (MPa)	$\sigma_{ult,x}$ (MPa)
30	1.25	7.62	12002 (25.2)	638 (33.0)	37.2	2.94
30	1.9	7.62	11812 (21.0)	444 (30.7)	36.4	3.37
30	2.5	7.62	12964 (24.2)	426 (36.4)	38.0	2.52
20	1.25	3.81	13646 (21.5)	366 (17.5)	42.8	2.25
20	1.9	3.81	12722 (13.6)	318 (41.2)	38.8	2.00
20	2.5	3.81	13729 (14.2)	415 (36.6)	36.8	2.17
20	1.25	7.62	13226 (31.9)	973 (35.4)	38.3	4.30
20	1.9	7.62	12461 (26.2)	703 (73.1)	36.7	3.75
20	2.5	7.62	12818 (25.7)	1080 (60.9)	39.4	4.29
10	1.25	3.81	11944 (29.3)	528 (21.6)	35.1	3.14
10	1.9	3.81	12843 (29.8)	496 (37.5)	36.7	3.15
10	2.5	3.81	12433 (23.7)	522 (22.3)	34.2	2.80
10	1.25	7.62	7918 (20.4)	1112 (28.3)	28.3	6.41
10	1.9	7.62	9345 (9.1)	1142 (40.4)	29.1	5.47
10	2.5	7.62	9333 (26.3)	946 (13.9)	27.7	5.33

Table 1: *Tensile Properties*

Length (cm)	Width (cm)	Vane Spacing (cm)	E_y (%COV) (MPa)	E_x (%COV) (MPa)	$\sigma_{ult,y}$ (MPa)	$\sigma_{ult,x}$ (MPa)
30	1.25	7.62	7596 (28)	587 (20)	27.6	4.67
30	1.9	7.62	8547 (30)	733 (39)	27.3	4.91
30	2.5	7.62	9014 (19)	496 (42)	27.3	4.94
20	1.25	3.81	9042 (27)	437 (21)	30.1	4.81
20	1.9	3.81	7910 (27)	444 (25)	25.8	4.50
20	2.5	3.81	9836 (19)	437 (40)	29.5	4.99
20	1.25	7.62	8068 (29)	969 (44)	25.2	5.55
20	1.9	7.62	8240 (22)	886 (23)	25.3	5.92
20	2.5	7.62	7771 (25)	694 (33)	24.6	5.90
10	1.25	3.81	8001 (20)	616 (29)	25.0	5.32
10	1.9	3.81	6627 (24)	774 (25)	21.7	7.01
10	2.5	3.81	9082 (32)	615 (26)	26.6	5.65
10	1.25	7.62	5642 (21)	1283 (36)	19.9	7.22
10	1.9	7.62	5072 (42)	1168 (22)	18.1	7.87
10	2.5	7.62	4832 (29)	1066 (31)	16.7	6.28

Table 2: *Compressive Properties*

The tension and compression properties for OSL panels in this study compare differently depending on the direction of loading. Tension properties are greater than compression in the parallel direction; however, no such difference exists for transverse properties (**Figure 4**, **Figure 5** and **Figure 6**). The literature, in general, discusses the difference in tensile and compressive properties based on σ_{ult} differences, without addressing E. For solid wood, parallel compressive strength is initiated by fiber bucking and is appreciably lower than the corresponding tensile value (Wangaard 1981). The stress-strain curves for this study illustrate a more pronounced non-linear response for compression than tension; possibly resulting from a difference in failure modes. Similarly, for fiber-reinforced composites, fiber fracture controls parallel tensile failure, while the corresponding compressive mode is fiber buckling (Jones 1975). The similarity in material performance across natural and synthetic composites supports the theory that different modes of failure influence the values of both E and σ_{ult} for uniaxial tests. Transverse values for tension and compression are closer and fail in modes different from parallel.

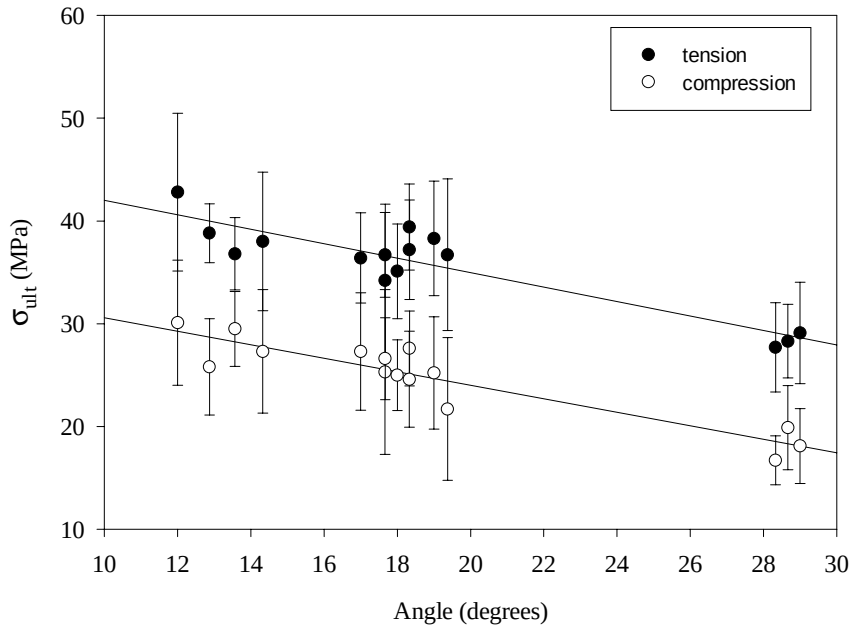

Figure 4: *Relationship between parallel strength and mean strand angle, assumed tensile gauge failure*

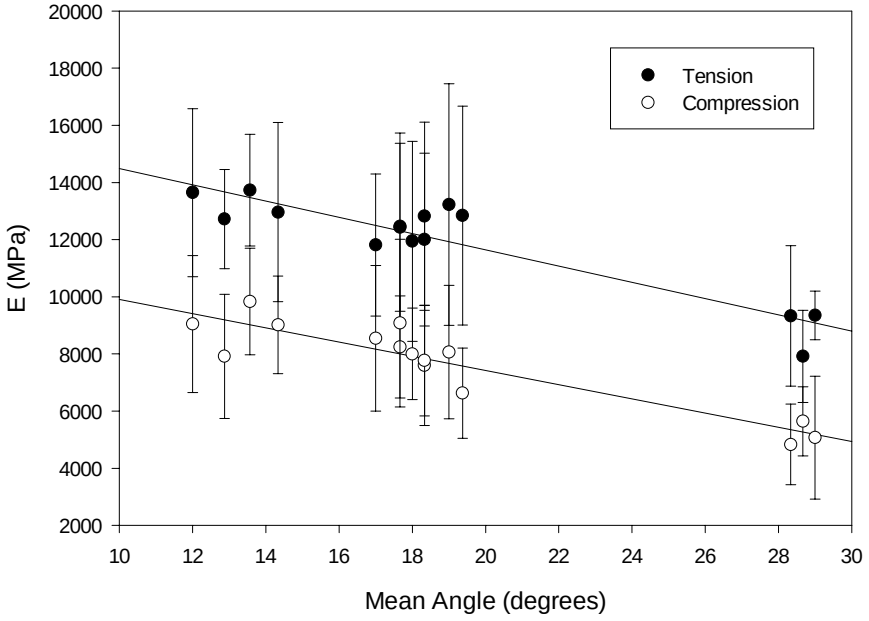

Figure 5: *Relationship between parallel E and mean strand angle*

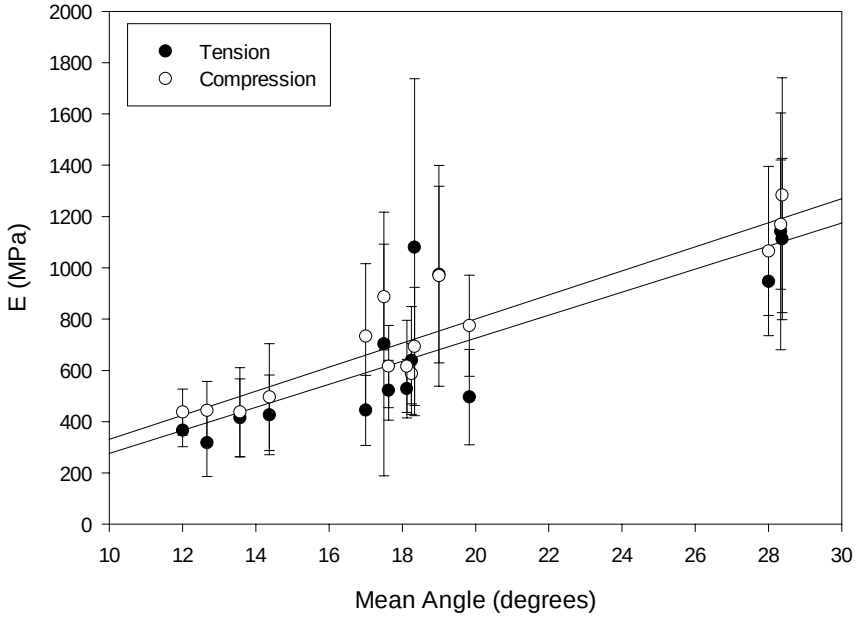

Figure 6: *Relationship between transverse E and mean strand angle*

Average internal bond (IB) values for all panel types ranged from 330 kPa to 585 kPa; all similar to the Canadian standard CSA 0437.0 which specifies an internal bond of 345 MPa for OSB products (Lowood 1997). Increasing strand length or width resulted in decreased IB (**Figure 7**). In contrast, panels with decreased levels of strand alignment and increased values of density displayed increased IB strengths.

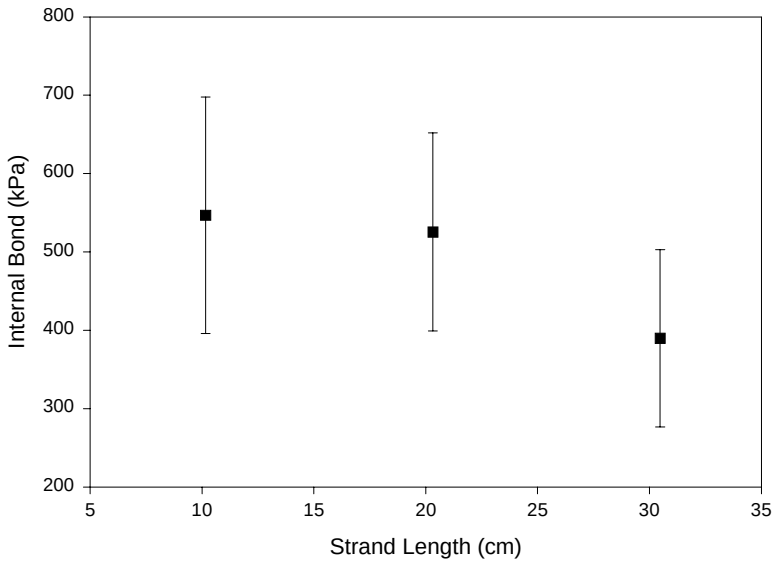

Figure 7: *Effect of strand length on IB*

Influence of Material Design Parameters

The statistical significance of density, mean strand angle, strand length, and strand width on E and σ_{ult} was determined using an ANOVA (**Table 3**). Density and mean angle both significantly influence nearly all of the properties. In general, neither length nor width directly control panel properties.

In general, strand geometry did not influence properties of the OSL, however, deviations from this general trend were observed (**Table 3**). Of particular note, both transverse tension E and strength exhibit dependence on strand length. Similarly, transverse compressive strength was also reliant on strand length. These results seem somewhat unusual because strand length lays nearly perpendicular to the direction of load, rather than strand width, which lies parallel to loading. Although no direct evidence is available, this result may imply that the correlation may result from a material structure parameter such as density variation or strand tilt out-of-plane of

the panel. It was noted that two out of the three transverse tension specimens for each panel were located along the panel edge, where density variation is often more prevalent.

p-values for Model Variables				
Response Variable	**Density**	**Mean Angle**	**Length**	**Width**
Parallel tensile E	**0.0030**	**<0.0001**	0.9266	0.7801
Transverse tensile E	0.1984	**<0.0001**	**0.0005**	0.2166
Parallel compressive E	**<0.0001**	**<0.0001**	0.5338	0.1668
Transverse compressive E	**<0.0001**	**<0.0001**	0.1307	0.5319
Parallel tensile strength	**<0.0001**	**<0.0001**	0.1859	0.6014
Transverse tensile strength	**<0.0001**	**<0.0001**	**0.0386**	0.5309
Parallel compressive strength	**<0.0001**	**<0.0001**	0.6716	0.5511
Transverse compressive strength	**<0.0001**	**<0.0001**	**<0.0001**	0.1823

Table 3: *Statistical significance of model variables (bold text denotes significance)*

Aligned strands form in patterns that result in varying high and low density regions. These forming issues appear to be intensified with longer strands. The mechanical alignment techniques seemed to readily form long strands into columns, between which lie low-density areas caused by large voids. It was noted that many of the transverse tension specimens failed at these low-density regions.

Despite the deviations mentioned previously, the statistical results illustrate the general independence of OSL properties on strand geometry. This is contrary to the results of many studies, possibly as a result of not separating the effects of strand geometry and orientation. Barnes (2000 and 2001) used strands from OSB lengths to OSL lengths and determined that increasing strand length increased composite properties. This behavior was modeled as a stress transfer angle using a modified version of the Hankinson equation. Wang and Lam (1999) studied panels with aligned faces and random cores using 5 to 10 cm strands. They determined that increasing strand slenderness ratio increased both MOR and MOE, however both panel density and strand orientation exhibited higher statistical significance than slenderness ratio. For

instance, doubling slenderness ratio from 83 to 167 only increased MOE and MOR ca. 11 and 16%, respectively.

A model developed by Simpson (1977) and data from a study performed by Suchsland (1968) observed improved strength properties for increasing slenderness ratios up to around 300, (i.e. a strand length of 23 cm for this study). Post (1958) found increasing properties with increasing length up to strands that are 10 cm long. Similarly, Brumbaugh (1960) tested panels with strand lengths of 1.25, 2.5, 5.0 and 10 cm and determined that increasing MOR resulted from use of longer strand lengths. Despite the corroborating results of these studies, none explicitly separated the effects of orientation and strand geometry within the experimental design, thereby complicating the ability to statistically separate strand geometry and orientation.

Although much of the literature places emphasis on the relationship between strand geometry and properties, some studies have found otherwise. Hoover *et. al*. (1992) found that for flakes of 5.0 and 7.5 cm long, length had no significant effect on MOR and MOE. Using a simulation analysis based on a volume-weighted rule of mixtures, Xu and Suchsland (1998) found no difference for MOE of simulated panels with two strand volumes.

In short glass and carbon fiber composites, critical fiber length is commonly used to determine the length of a fiber needed to adequately transfer stress between the fiber and matrix, ensuring failure in the fiber rather than the matrix. For a rectangular reinforcing element such as a strand, critical strand length (l_c) is defined by.

$$l_c = \frac{\sigma_{fu}}{\tau_y\left(\frac{1}{b}+\frac{1}{a}\right)}$$ Equation 2.1

where b is the strand width, a is the strand thickness, σ_{fu} is ultimate fiber stress and τ_y is the matrix or between fiber yield shear stress. This relationship assumes that the stress at the end of

the fiber is negligible and that the matrix is rigid and perfectly plastic meaning that the shear stress in the matrix is constant along the fiber length. The critical fiber length was calculated using Equation 2.1 to yield a parallel critical fiber length of approximately 0.05 cm and a transverse length of less than 0.003 cm. The critical lengths calculated do not require the lengths that much of the literature cites as necessary, but support the finding that for the lengths tested, fiber length does not directly influence properties.

An ANOVA was used to determine the influence of mean angle, density, length and width on IB values. All factors were found to be statistically significant. Tukey's comparison test was used to determine the mean IB for the 30 cm strand specimens is different from the means for the 10 and 20 cm strand specimens (**Figure 7**). The 2.5 cm width was statistically different from the 1.25 and 1.9 cm widths which are the same. The dependence of IB on strand length could be a result of more variable material structure for the longer strands in the form of larger individual voids and increased column effects.

In Plane Angle

In plane strand orientation is a major factor affecting composite properties. For oriented strand composites, it is measured as the angle between the long axis of the strand and the panel axis parallel to the preferred strand orientation. Mean angle is calculated as the average of the absolute value of multiple measures of strand angle and is used as a deterministic descriptor for the variable strand orientation within a panel. Values of parallel E and strength increase with higher levels of orientation (McNatt *et. al.*1992, Wang and Lam 1999). Even small angles of orientation are important, as the first 20 degrees of off-axis alignment can reduce properties to near half of aligned properties (Wood Handbook 1987). Out of plane angle of strands has also

been identified as important variable in oriented strand composites but for simplicity was not considered in this research (Xu and Suchsland 1998).

Mean angles were calculated for each of the panel types (i.e. length, width and vane spacing combination). The dependence of this variable on vane spacing, length and width was determined using an ANOVA. Both length and vane spacing significantly influence mean angle (**Table 4**). Differences in orientation as a result of strand length were determined using Tukey's test. The 30 cm and 20 cm strands have similar orientation classes, but are both different from the 10 cm strands. However, the strand width did not appear to have a statistically significant influence on the mean angle.

Variable	Degrees of Freedom	F-value	p-value
Model	5	77.75	<0.0001
Vane spacing	1	187.36	<0.0001
Strand length	2	135.52	<0.0001
30 cm (A)			
20 cm (A)			
10 cm (B)			
strand width	2	0.76	0.473

Table 4: *ANOVA determining factors influential on mean angle, A and B represent different levels of orientation between length classes*

The non-linearity of off-axis orientation effects on mechanical properties has inspired many researchers to describe orientation data with statistical distributions (Harris and Johnson 1982, Shaler and Blankenhorn 1990, Shaler 1991, Wang and Lam 1999). Comparing the orientation of two panels to determine if the degree of alignment is statistically identical is more accurate when assessing the entire distribution rather than just the mean angles.

Angular data for distributions within a strand length class found to be statistically similar were combined. Interpretation of the mean angle analysis indicated that orientation varied with vane spacing and length. The K-S tests on angular distributions were used to validate the results that width has no statistical effect on orientation over the all panel types. This result held for the

10 and 20 cm strand length. Therefore, the distributions were combined across widths for a the 10 and 20 cm lengths within a vane spacing. The angular distributions for the 30 cm strands, however, were influenced by strand width. Multiple pair-wise comparisons for the remaining groups were performed and the results are given in **Table 5**.

The K-S test identifies distributions as distinct for p-values less than 0.10. Three sets of distributions are statistically the same and are denoted with bold type in **Table 5**: the 10 cm at 3.8 cm spacing was combined with the 20 cm at the 7.6 cm spacing, the 20 cm stands at 7.6 cm spacing was combined with the 30 x 1.25 cm strands, and the 20 cm strands at the 3.8 cm spacing with the 30 x 2.5 cm strands. These sets of distributions, shown in **Table 5** with bold p-values, were combined. The combined distributions should have nearly identical properties as geometry has no effect outside of orientation, and with a single target density should reduce differences by density to minimal levels. The similar parallel tensile properties for these values are illustrated by **Figure 8**.

units are cm		vane spacing	3.81		7.62				
		length	10	20	10	20	30		
vane spacing	length	width	all	all	all	all	1.25	1.9	2.5
3.81	10	all	1	<0.0001	<0.0001	**0.1026**	0.0175	0.0580	0.0009
	20	all	-	1	<0.0001	<0.0001	0.0009	0.0003	**0.3329**
7.62	10	all	-	-	1	<0.0001	<0.0001	<0.0001	<0.0001
	20	all	-	-	-	1	**0.3536**	0.0079	0.0105
	30	1.25	-	-	-	-	1	0.0069	0.0294
		1.9	-	-	-	-	-	1	0.0235
		2.5	-	-	-	-	-	-	1

Table 5: *p-values from Kolmgorov-Smirnov 2-sample test, all lengths are in cm and all distributions that are the same are in bold type*

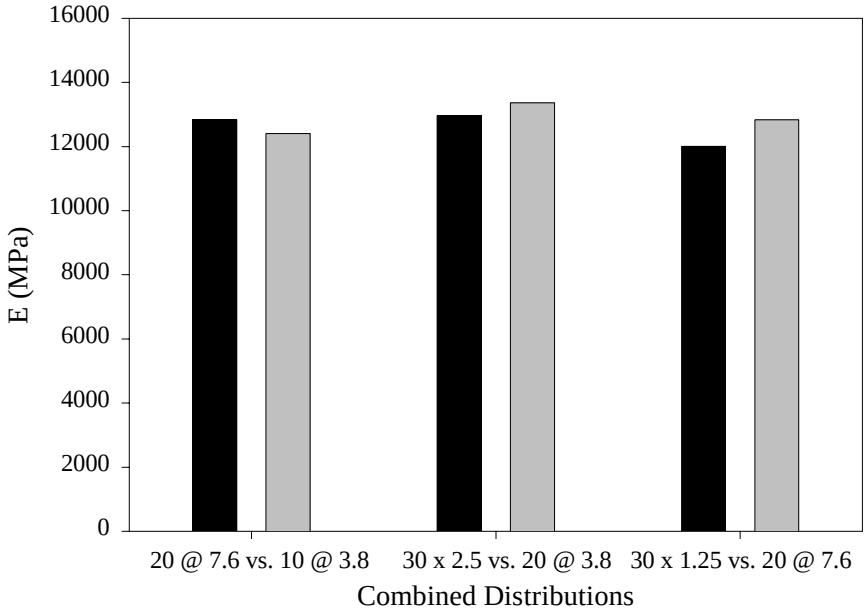

Figure 8: *Parallel tensile property comparison for test cells with same angular distributions (lengths and vane spacings in cm)*

CONCLUSIONS

Using an ANOVA considering strand length, width, mean strand angle and composite density, the dominant parameters controlling mechanical properties are strand orientation and composite density. However, a separate analysis indicated strand length facilitated alignment with the mechanical orienter used in this study. The independence of mechanical properties on strand geometry could allow for the use of shorter strands in structural composite lumber if adequate alignment is achieved. Previous work, citing strand length as necessary for good mechanical properties studied strands with lengths below the range investigated where length may directly influence properties. In addition experimental designs that do not consider multiple levels of both strand geometry and orientation may have difficulties separating effects. OSB length strands may be used to achieve structural properties characteristic to OSL, however alignment must be adequately controlled. For instance, in our study composites produced with

10 cm strands with a high degree of alignment achieved an average E_y and a $\sigma_{ult,y}$ of 12407 MPa and 35 MPa, respectively. Continued development is necessary to economically align OSB strands in a plant environment.

REFERENCES

ASTM 1996. *Standard Methods for Mechanical Properties of Lumber and Wood-Base Structural Material*. Standard D4761-96. American Society of Testing and Materials.

ASTM 1998. *Standard Specification for Evaluation of Structural Composite Lumber Products*. Standard D5456-98a. American Society of Testing and Materials.

ASTM 1998. *Standard Test Method for Compressive Properties of Rigid Plastics*. Standard D695-96. American Society of Testing and Materials.

ASTM 1997. *Standard Test Methods for Direct Moisture Content Measurement of Wood and Wood-Base Materials*. Standard D4442-92. American Society of Testing and Materials.

ASTM 1997. *Standard Test Methods for Evaluating Properties of Wood-Base Fiber and Particle Panel Materials*. Standard D1037-96a. American Society of Testing and Materials.

Barnes, Derek. *An Integrated Model of the Effect of Processing Parameters on the Strength Properties of Oriented Strand Wood Composites*. Forest Products Journal. 50(11/12), 2000. pp. 33-42.

Barnes, Derek. *A Model of the Effect of Strand Length and Strand Thickness on the Strength Properties of Oriented Wood Composites.* Forest Products Journal. 51(2), 2001. pp. 36-46.

Brumbaugh, James. *Effect of Flake Dimensions on Properties of Particle Boards*. Forest Products Journal. May 1960. pp. 243-246.

Geimer, Robert L., Kent A. McDonald, Friend K. Bechtel and James E. Wood. *Measurement of Flake Alignment in Flakeboard with Grain Angle Indicator*. Research Paper FPL-RP-518. 1993.

Harris, Robert A. and Jay A. Johnson. *Characterization of Flake Orientation in Flakeboard by the von Mises Probability Distribution Function*. Wood and Fiber. 14(4), 1982. pp. 254-266.

Hoover, William L., Michael O. Hunt, Robert C. Lattanzi, James H. Bateman, John A. Youngquist. *Modeling Mechanical Properties of Single-Layer, Aligned, Mixed-Hardwood Strand Panels*. Forest Products Journal. 42(5). 1992. pp. 12-18.

Jones, Robert M. *Mechanics of Composite Materials*. McGraw-Hill Book Company. 1975. pp. 128-135.

Knudson, R.M. *PSL 300^{TM} LSL: The Challenge of a New Product*. Proceedings of the Twenty-

Sixth Washington State University International Particleboard/Composite Materials Symposium. 1992. Pp. 206-214.

Lehmann, W.F. *Properties of Structural Particleboards*. Forest Products Journal. January 1974 24(1). pp. 19-26.

Linville, Jeffery D. *The influence of a horizontal density distribution on moisture-related mechanical degradation of oriented strand composites*. Master's Thesis. Washington State University. 2000.

Lowood, John. *Engineered Wood Products: A Guide for Specifiers, Designers and Users; Chapter 5: Oriented Strand Board and Waferboard*. PFS Research Foundation. 1997. pp. 5-133.

McNatt, J. Dobbin, Lars Bach and Robert W. Wellwood. *Contribution of flake alignment to performance of strandboard*. Forest Products Journal. March 1992. 42(3). pp. 45-50.

Meyers, Kristin. *Modeling of oriented strand composites based on strand geometry and orientation for single layer panels: Appendix*. Master's Thesis. Washington State University. 2001.

National Research Council Canada. *CCMC Evaluation Report: TimberStrand® LSL*. February 2001. pp. 1-4.

Nelson, Sherman. Engineered Wood Products; A Guide for Specifiers, Designers and Users: Chapter 6 - Structural Composite Lumber. pp 6-147 to 6-172. 1997 PFS Research Foundation. Madison, WI.

Ostle, Bernard and Linda C. Malone. *Statistics in Research: Basic Concepts and Techniques for Research Workers*; *Fourth Edition*. Iowa State University Press. Ames, Iowa. 1998. pp. 66-67.

Post, P.W. *Effect of Particle Geometry and Resin Content on Bending Strength of Oak Flake Board*. Forest Products Journal. October 1958. pp. 317-322.

Shaler, S.M. *Comparing Two Measures of Flake Alignment*. Wood Science and Technology. 26, 1991. pp. 53-61.

Shaler, Stephen M. and Paul R. Blankenhorn. *Composite Model Prediction of Elastic Moduli for Flakeboard.* Wood and Fiber Science. 22(3), 1990. pp. 246-261.

Simpson, William T. *Model for Tensile Strength of Oriented Flakeboard*. Wood Science. 10(2), October 1977. pp.68-71.

Suchsland, Otto. *Particle-Board From Southern Pine*. Southern Lumberman. December 1968. pp. 139-144.

Triche, Michael H., and Hunt, Michael O. *Modeling of Parallel-Aligned Wood Strand Composites.* Forest Products Journal. Vol. 43 #11/12 1993. pp. 33-44.

Wang, Kaiyuan and Lam, Frank . *Quadratic RSM Models of Processing Parameters for Three-layer Oriented Flakeboard.* Wood and Fiber Science. April 1999, 31(2). pp. 173-186.

Wangaard, F.F. *WOOD: Its Structure and Properties*. Educational Modules for Material Science and Engineering. University Park, PA. 1981. pp. 249-250.

Wood Handbook #72 1987.U.S. Forest Products Laboratory, pp 4-14, 4-25, 4-29.

Xu, Wei and Suchsland, Otto. *Modulus of Elasticity of Wood Composite Panels with a Uniform*

CHAPTER 3

EVALUATING DESIGN PROCEDURES FOR THE ELASTIC MODULUS OF ORIENTED STRAND COMPOSITES

ABSTRACT

Existing relevant models in the literature used to design or predict elastic properties of oriented strand composites are in general fully or semi-empirical. These models predict properties well within the bounds of applicability set by the data modeled. However, in order to develop a more widely applicable model, a mechanics of materials approach was evaluated in addition to verifying existing semi-empirical models. Test data was compared with predicted values from a model developed by Barnes (2000), the Hankinson equation and tensor transformation, using either the mean angle or a the rule of mixtures (ROM) in combination with a distribution of angles. Barnes' model predicted properties best on average for the range of data used, although tensor transformation and ROM in conjunction with the normal distribution predicted properties nearly as well with more consistency.

INTRODUCTION

Design of wood-strand composites has focused mainly on describing property trends observed from empirical research. Statistical models for oriented strand composites have been developed with some success, however, these models are generally too explicit to be widely applicable. Empirical models fit specific data well and can predict properties accurately, but are limited to the range of data tested. Some mechanical models have been developed with a combination of theoretical and statistical methods. Unfortunately these efforts often do not cover

the scope of strand geometries used in commercial applications. A more fundamental model could be used for any range of geometries to predict properties. Thus, a fundamental design procedure validated for strand composites over a large spectrum of geometries is needed.

Triche and Hunt (1993) developed a finite element (FE) model to predict tensile properties of oriented strand composites. Avoiding the difficulties of modeling properties of adhesive joints, each strand and the corresponding resin interface was represented in the FE program as a single superelement. Utilizing this process to model an entire panel, the element structure would be repeated, limiting the variability, inherent in strand composites. This model is versatile with respect to inputs, but the current errors are varied between excellent and poor. In addition, the data used to assess the model was from small, hand laid, perfectly oriented panels.

In contrast, multiple statistical models have been developed by fitting regression models to specific empirical data sets. Hoover *et al*. (1992) developed regression models to relate various panel properties to strand length and thickness, board density, and an alignment factor found using stress-wave timing. The models were limited to strands that were either 5.1 or 7.6 cm long and either 0.038 or 0.064 cm thick. Predicting properties with varying success, the models described parallel tensile modulus to within 10% of actual values with a COV of 56.2%. Likewise, Lehmann (1974) developed a model with similar variables for flakes of shorter lengths (1.25 to 5.1 cm) achieving an r^2 value of 0.878. A common difficulty with using or comparing these and other empirical models is that much of the literature only discusses general trends without actually quantifying the data into a set of predictive equations that are general enough to apply outside the specific study.

Finally, semi-empirical models combine fundamental mechanics descriptions of the material system with empirical descriptions of different attributes. Xu and Suchsland (1998) used energy methods to develop a volume-based rule of mixture (ROM) to predict the composite elastic moduli (E) from the anisotropic mechanical properties of wood and distribution of particle orientation. The ROM is a weighted average used to model the combination of different materials arranged in parallel. Xu and Suchsland combined this expression with Hankinson's equation to account for strand orientation effects for a simulation study, no comparison was drawn between test data and simulated properties.

Using a different approach, Barnes (2000) developed a model that modifies solid wood properties to account for panel density, in-plane strand orientation, strand length and thickness, fines content, and adhesive content. This model was developed using a wide range of material and manufacturing variables, allowing for more general application of the model. Percent deviation of the measured mean modulus of elasticity (MOE) from the predicted MOE for strands 4.2 to 8.0 cm ranged from –9.2 to 7.9%.

OBJECTIVES

Modeling of strand products is often accomplished through empirical relationships that model exact data over a specific range and therefore fail to provide information on materials outside this range. While developing an effective design procedure for oriented strand composites, the specific objectives of this research are to:

1. Independently validate current semi-empirical material design methods predicting E.
2. Establish separate, fundamental mechanics methods for discerning the predictive role of strand orientation.
3. Evaluate and compare the various design methods over a range of strand geometries.

ANALYTICAL DEVELOPMENT

One of the current design models for oriented strand products, developed by Barnes (2001), relates many of the panel attributes to properties with good success. However, this method is highly empirical and has not been independently validated past the data range used to develop many of the model parameters, especially those used in accounting for strand orientation using Hankinson's equation. Xu and Suchsland (1998) have simulated the elastic response of wood composite panels using the parallel ROM. This research did not evaluate effectiveness by comparing simulated properties with test data. This approach describes the strand orientation effect using the entire distribution of strand orientation rather than a single mean panel angle, defined as the average of the absolute values of the angles the strands form with the strong panel axis. In accounting for strand orientation, this approach can rely the empirical Hankinson equation or the well founded tensor transformation.

Semi-Empirical Method

Barnes (2001) proposed a semi-empirical design procedure for oriented strand composites that modifies solid wood properties for a variety of composite design and manufacturing parameters. In its simplest form, the procedure for determining the composite modulus (E_c) from the solid wood modulus (E_w) can be reduced to:

$$E_c = E_w k_a k_f k_\rho k_\theta k_g \qquad \text{Equation 3.1}$$

where k are correction factors and subscripts a, f, ρ, θ, g denote adhesive content, fines content, panel density, mean strand orientation, and strand geometry, respectively. In addition, subscripts c and w denote the composite and solid wood materials, respectively.

The influence of manufacturing parameters such as percent resin (r) and fines content in percent (x) are considered through:

$$k_a = 1 - \frac{1}{e^{0.8 \cdot r}}$$ Equation 3.2

$$k_f = 1 - (E_w - E_f)x$$ Equation 3.3

Barnes assumes elastic properties to scale linearly with density, therefore:

$$k_\rho = \frac{\rho_c}{\rho_w}$$ Equation 3.4

The influence of strand orientation is assumed to follow Hankinson's equation using a the mean angle.

$$k_\theta = \frac{E_w^t}{E_w^l\left(\sin^n\theta\right) + E_w^t\left(\cos^n\theta\right)}$$ Equation 3.5

Where superscripts *l* and *t* denote the longitudinal and transverse directions for solid wood properties. Barnes noted that the adjustable exponent, *n*, did not equal typical values. Instead he constructed a linear regression of empirically derived exponent values for different strand thicknesses. For the in-plane strand orientation effects, *n(θ)* can be computed from original strand thickness (*d*, *given in inches*) as:

$$n(\theta) = 3.3 - 12\left(d\frac{\rho_w}{\rho_c}\right)$$ Equation 3.6

The mean strand angle can be measured on panels or predicted as a function of orienter to mat spacing (*h*), strand length (*L*), and the vane spacing (*s*) in inches as:

$$\theta = \frac{\sin^{-1}(s/L)}{2} + h(4.87 - 0.377L)$$ Equation 3.7

Strand length (*L*) and thickness (*d*) are assumed to alter panel properties and are considered through a stress transfer angle:

$$\phi = \tan^{-1} \frac{2d\rho_w}{L\rho_c}$$ Equation 3.8

which is then considered using Hankinson's equation:

$$k_g = \frac{E_w^t}{E_w^l \left(\sin^n \phi\right) + E_w^t \left(\cos^n \phi\right)}$$ Equation 3.9

In turn, $n(\phi)$ can be computed using:

$$n(\phi) = 0.95 + 2.38\left(d\frac{\rho_w}{\rho_c}\right)$$ Equation 3.10

All of the empirical equations are based on English units. The values discussed later were predicted in psi and converted to MPa.

Mechanics of Materials Models

Xu and Suchsland utilized a ROM approach for considering particle orientation in oriented strand board (OSB). The strand volume fraction (V_θ/V) for each angle θ, may be reduced to the probability value of that angle ($P(\theta)$) by assuming that strands are of equal volume:

$$E_c = \sum \frac{V_\theta E_\theta}{V} = \sum P(\theta) E_\theta$$ Equation 3.11

Although Xu and Suchsland used the von Mises distribution for $P(\theta)$ of the single layer (OSB), other distributions were considered. The angular distributions used to describe the surface orientation in panels include the beta, von Mises, normal and 2-parameter Weibull distributions (Xu and Suchsland 1998, Harris and Johnson 1982, Shaler 1991 and Wang and Lam 1999). When using the 2-parameter Weibull distribution, $P(\theta)$ can be described as:

$$P(\theta) = \frac{\beta}{\lambda}\left(\frac{\theta}{\lambda}\right)^{\beta-1} \exp\left[-\left(\frac{\theta}{\lambda}\right)^{\beta}\right] \quad for\ \theta > 0 \qquad \text{Equation 3.12}$$

where: λ and β represent the scale and shape factors; respectively (Kettegoda and Rosso).

In contrast, the orientation under a normal distribution can be expressed as:

$$P(\theta) = \frac{1}{\sigma\sqrt{2\pi}} \cdot \exp\left[-\frac{1}{2}\left(\frac{\theta-\mu}{\sigma}\right)^{2}\right] \quad for\ -\infty < \theta < \infty \qquad \text{Equation 3.13}$$

where: μ and σ represent the mean and standard deviation; respectively (Kettegoda and Rosso).

Computing the influence of off-axis orientation (θ) on E can be performed using either Hankinson's equation or tensor transformation. Given the elastic moduli in the principal material directions (E_1 and E_2), either method can be effectively used to predict the composite material properties, E_y and E_x (**Figure 9**). However, the empirical Hankinson equation requires an adjustable parameter, *n*, to be known *a priori*.

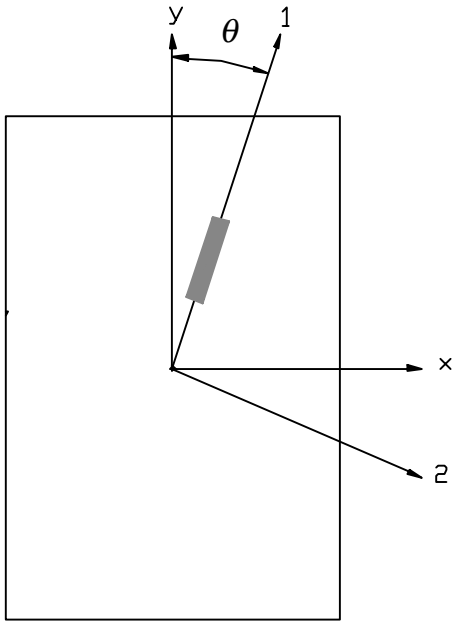

Figure 9: *Explanation of material coordinates as compared to composite coordinates*

Hankinson Equation

For panel design, the Hankinson equation is most commonly used in conjunction with a mean angle (Equation 5). For the semi-empirical method described previously, Barnes describes the method for obtaining a suitable exponential constant, *n*. However, this approach combines both the empirical adjustments necessary using mean angle with that for the Hankinson equation. Using the Hankinson equation with the entire distribution for strand orientation, would call for a different exponential constant. The Wood handbook recommends a value of 2.0 for *n*, when considering MOE. To avoid specifically fitting the Hankinson equation to off-axis elastic constants, $n = 2.0$ will be considered throughout this work.

Tensor Transformation

Alternatively, tensor transformation introduces a mechanics of materials method to compute orientation effects on elastic constants of anisotropic materials. Defining the compliance matrix, S, and the transformation matrix, T, for orthotropic materials as:

$$S = \begin{bmatrix} \frac{1}{E_1} & \frac{-\nu_{12}}{E_1} & 0 \\ \frac{-\nu_{12}}{E_1} & \frac{1}{E_2} & 0 \\ 0 & 0 & \frac{1}{G_{12}} \end{bmatrix} = \begin{bmatrix} S_{11} & S_{12} & 0 \\ S_{12} & S_{22} & 0 \\ 0 & 0 & S_{66} \end{bmatrix} \qquad \text{Equation 3.14}$$

$$T = \begin{bmatrix} c^2 & s^2 & 2 \cdot sc \\ s^2 & c^2 & -2 \cdot sc \\ -sc & sc & c^2 - s^2 \end{bmatrix} \qquad \text{Equation 3.15}$$

Where E_1 and E_2 are elastic moduli in the principal material directions, ν_{12} is the Poisson's ratio, G_{12} is the modulus of rigidity, and s and c are the sine and cosine of the angle, θ; respectively. The transformed compliance matrix ($\overline{S}$) is represented as:

$$\bar{S} = T^T S\, T \qquad \text{Equation 3.16}$$

The value for E_θ is then computed using:

$$E_\theta = \frac{1}{\overline{S_{11}}} = \frac{1}{S_{11}\cos^4(\bar{\theta}) + (2S_{12} + S_{66})\sin^2(\bar{\theta})\cos^2(\bar{\theta}) + S_{22}\sin^4(\bar{\theta})} \qquad \text{Equation 3.17}$$

With $\bar{\theta}$ is the mean angle for E_y and the mean angle plus 90° for E_x.

Distributions

The tensor transformation equation and the Hankinson equation as stated in Equations 3.17 and 3.5 use a single, deterministic value for a mean angle. This approach would be more appropriate if orientation affected properties in a linear manner or if the strands were aligned in a single direction. However, this was not the case. To evaluate the error introduced by using a mean angle, transformation using both the normal and 2-parameter Weibull distributions were evaluated (Meyers 2001a).

The E at the center of each bin was calculated using the Hankinson equation along with the corresponding probabilities by integrating $P(\theta)$ for either the Weibull or normal distribution. The transformed E is defined as:

$$E_c = \sum_{n=1}^{180/\Delta\theta} \left[\left[\int_{(n-1)\Delta\theta}^{n\Delta\theta} P(\theta) \right] \cdot \left[\frac{E_1 \cdot E_2}{E_1 \sin^2(\theta) + E_2 \cos^2(\theta)} \right]_{(n\Delta\theta - \Delta\theta/2)} \right] \qquad \text{Equation 3.18}$$

The same procedure was then applied to tensor transformation to obtain:

$$E_c = \sum_{n=1}^{180/\Delta\theta} \left[\left[\int_{(n-1)\Delta\theta}^{n\Delta\theta} P(\theta) \right] \cdot \left[\frac{1}{\overline{S}_{11}} \right]_{(n\Delta\theta - \Delta\theta/2)} \right] \qquad \text{Equation 3.19}$$

Utilizing the entire distribution of angles was accomplished by dividing the range of angles, 0 to π radians, into 18 bins. The bin width, Δθ, of π/18 radians was evaluated through a sensitivity analysis (**Figure 10**). The effect of the width of Δθ was determined through this

analysis. Smaller width will increase accuracy at decreasing rates, while increasing computational difficulty. Therefore, a balance between accuracy and ease in calculations has to be found. This occurs for the smaller widths as the curve shown in **Figure 10** levels off around the value chosen for $\Delta\theta$.

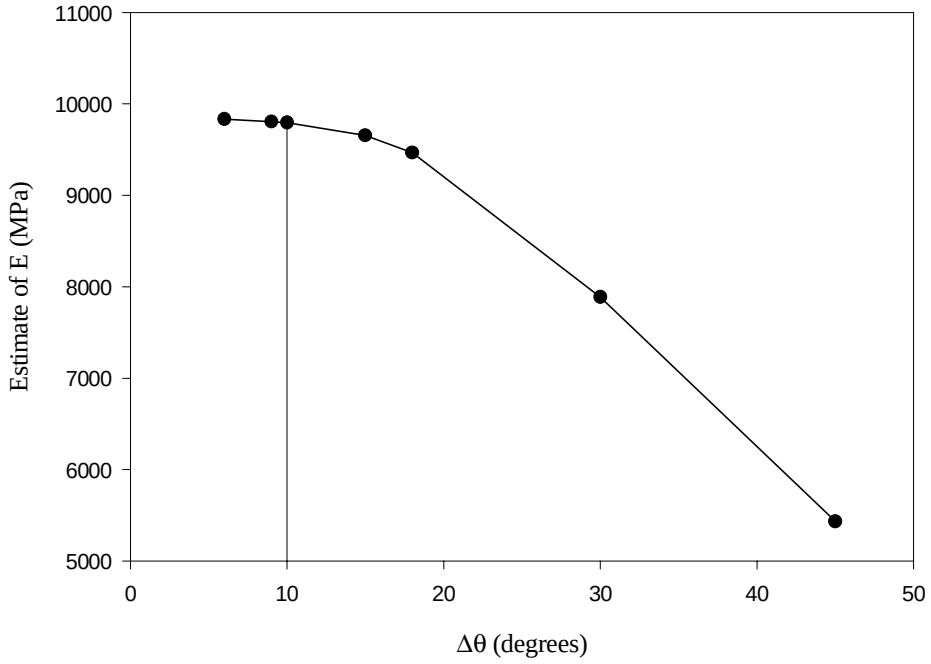

Figure 10: *Sensitivity analysis of bin width*

RESULTS AND DISCUSSION

Strand Properties

Tension tests were performed by Vikram Yadama to determine E_1, E_2, ν_{12} and G_{12} of individual strands conditioned to the same conditions as panels (Meyers 2001a). The in-plane grain angle of each strand was used in conjunction with the displacements, loads, and tensor transformation equations to solve for these approximations of principal material properties

(**Table 6**). Few comparative studies are available in the literature, but Triche and Hunt (1993) obtained a similar value of parallel tensile E, 11721 MPa, from veneer strand tests.

Density (kg/m^3)	E_1 (MPa)	E_2 (MPa)	G_{12} (MPa)	ν_{12}
Strand (390)	11866	594	656	0.49
Elevated (640)	19374	969	1071	0.49

Table 6: *Measured and elevated strand properties*

The panel density was higher than that of the strands. Comparison of transformed strand properties and measured panel properties necessitates the strand properties be changed to reflect panel density. The average density of the strands was 390 kg/m^3, while the panel test specimens averaged 640 kg/m^3. The effect of increased density on mechanical properties has been the subject of many studies and has been identified as elevating these properties. Bodig and Goodman (1973) correlating the difference in density between species to property variation through Equation 3.20.

$$y = ax^b \qquad \text{Equation 3.20}$$

Where y is the property at the new density level, a is the initial property, x is the ratio of the desired to initial density and b is an empirical factor.

Bodig and Goodman found that for Young's moduli and moduli of rigidity b ranges from 1.07 to 1.26 and nears zero for Possion's ratio. Palka (1973) found that Young's moduli have an exponent of 1.0 and the exponent for Possion's ratio varies between –1 and 1 with principal directions for softwoods. The relationship between density and both the Young's and rigidity moduli are linear, yielding a b of 1, according to Kellogg and Ifju (1962). Most of these studies produced exponents near 1 for E and G and around zero for Possion's ratio. Thus, $b = 1$ was used in modifying the strand properties to elevated densities (**Table 6**).

Validation of Barnes' Model

Barnes' model, as outlined above, relies on multiple factors multiplied by a solid sawn wood property value to prediction of E_θ. The factor defined to account for fines was not considered in this study as the fines were eliminated from each panel leading to $k_f = 1.0$. The adhesive and density factors were constant for all panels at 0.992 and 1.63, respectively. The factors calculated to adjust for strand length for a strand lengths of 10, 20 and 30 cm the factors were 0.841, 0.914 and 0.941, respectively. The most significant modifications in E_θ were from k_ρ and k_θ, with less influence from k_g and k_a.

The method defined by Barnes (2001) was completed with two values of mean angle; the measured angles from the experimental panels and the mean angle predicted using Barnes' relationship (Equation 3.7). Prediction of mean angle using this model has two parts. One relies on the height of the orienter above the mat, which was assumed constant at 5.1 cm. The other based on vane spacing, both of these factors also rely on strand length.

Barnes' model predicted parallel values well, the best predictions are shown with bold type, when using a measured mean angle (**Table 8**). Values obtained from testing were used in calculation of percent error of predictions (**Table 7**). The accuracy was not as good for values calculated using the predicted mean angle (**Table 8**). The empirical relationships were developed using parallel values therefore, transverse properties were not predicted. The inability to predict transverse properties illustrates the need for a more fundamental and thus, independent model.

Strand Length (cm)	30	20	30	30	20	20	10	10
Stand Width (cm)	1.25	all	1.9	2.5	all	all	All	All
Vane Spacing (cm)	7.6	3.8	7.6	7.6	3.8	7.6	3.8	7.6
Parallel Tensile E (MPa)	12627		11812	13265		12621		8865
Parallel Compressive E (MPa)	7929		8547	8979		7730		5182
Transverse Tensile E (MPa)	849		444	381		717		1067
Transverse Compressive E (MPa)	773		651	454		747		1155

Table 7: *Elastic moduli determined from testing*

Strand Length (cm)	10		20		30
Vane Spacing (cm)	3.8	7.6	3.8	7.6	7.6
Predicted $\bar{\theta}$ (degrees)	17.7	31.0	9.11	14.7	7.93
Measured $\bar{\theta}$ (degrees)	18.3	28.5	12.6	18.4	16.8
% Error in $\bar{\theta}$	3.28	-8.77	27.7	20.1	52.8
% Error Using Predicted $\bar{\theta}$	16.3	43.4	-27.4	-14.3	-45.0
% Error Using Measured $\bar{\theta}$	**2.78**	**33.0**	**-18.1**	**4.01**	**-12.3**

Table 8: *Percent error for predicted parallel tensile E (MPa) and mean angle using Barnes model by strand length and vane spacing (cm)*

Role of Orientation in Prediction of E

Probability Density Functions

Strand orientation was quantified through measurements of the strands angles on the panel face. Details of the procedure used to measure strand angles are in (Meyers 2001b). The angular data can be described using a variety of distribution types. The beta distribution is best suited for skewed data, which is not represented in the panels studied. The von Mises distribution was developed for angular data, but relies on one parameter and does not provide enough flexibility for a proper fit to the panel data. The 2-parameter Weibull and the normal distributions, both provide adequate fit to the experimental data and were utilized to describe the angles (Meyers 2001a). The probability density function (pdf) for the 2-parameter Weibull is defined by Equation 12. To accommodate the restriction on the Weibull distribution of using only positive values, $\pi/2$ radians was added to all measured angles to give a range of angles from 0 to π degrees. These angles were used for both distributions for consistency. Equation 13 is the

probability density function for the normal distribution. The 2-parameter Weibull and the normal distributions fit the data well. Distribution parameters and goodness of fit statistics are shown in **Table 9**.

GROUP	NORMAL DISTRIBUTION					WEIBULL DISTRIBUTION			
	PARAMETERS		FIT STATISTICS (p-value)			PARAMETERS		FIT STATISTICS (p-value)	
	MEAN	STDEV	Cramer-von Mises	Anderson-Darling	Skewness	SCALE	SHAPE	Cramer-von Mises	Anderson-Darling
30 x 1.25 plus 20 @ 7.26	89.4	19.1	<0.0050	<0.0050	-0.077	96.8	4.8	<0.010	<0.010
30 x 1.9	91.0	22.8	<0.0050	<0.0050	-0.289	99.5	4.4	<0.010	<0.010
30 x 2.5 plus 20 @ 3.81	89.8	17.8	<0.0050	<0.0050	0.183	96.9	5.0	<0.010	<0.010
10 @ 7.62	90.2	35.2	<0.0050	<0.0050	0.014	100.9	2.7	<0.010	<0.010
20 @ 7.62 plus 10 @ 3.81	90.0	23.7	<0.0050	<0.0050	-0.056	98.7	4.1	<0.010	<0.010

Table 9: *Distribution parameters and goodness of fit statistics*

Transformation Results

Transformation of E was completed using a variety of methods. Both the Hankinson equation, with the recommended $n = 2.0$, and tensor transformation were utilized in conjunction with a mean angle or the either the normal or Weibull distribution and the ROM for both panel directions. Of these methods, the most accurate predictor of parallel tensile E is tensor transformation using the normal distribution and ROM. Compressive parallel E, which is lower than tensile parallel E, was predicted best using tensor transformation and the mean strand angle. Compressive E could be influenced by failure mechanisms other than compression. In addition, the effect of pre-existing defects on a compression sample behavior could explain the reason values obtained in testing are lower than the predicted values. Mean angles, for both the Hankinson equation and tensor transformation, consistently under-predict tensile E_y. The percent error of the predicted to actual parallel tensile E values are contained in **Table 10** with

the most accurate prediction highlighted with bold type. Errors in predictions may be a result of input strand properties or the assumptions of the ROM.

Strand Length (cm)		30	20	30	30	20	20	10	10
Stand Width (cm)		1.25	all	1.9	2.5	all	all	all	All
Vane Spacing (cm)		7.6	3.8	7.6	7.6	3.8	7.6	3.8	7.6
Tensor Transformation	Normal	**11.0**		**17.1**	**13.0**		**22.5**		14.9
	Weibull	18.8		19.4	21.6		26.1		**14.1**
	Mean	39.8		29.5	18.1		39.3		52.8
Hankinson	Normal	16.2		22.1	17.9		27.3		20.5
	Weibull	23.9		24.8	26.5		31.2		22.7
	Mean	46.9		37.7	25.9		46.6		58.9

Table 10: *Percent Error predicted to measured tensile parallel E using multiple methods (bold type denotes best prediction)*

Transverse E was not predicted as well as parallel E. All transverse predictions were above the measured tensile and compressive values (**Table 11**). However, the most accurate method of prediction used mean strand angle and Hankinson's equation with n = 2.0, shown in bold text in **Table 11**. The effectiveness of tensor transformation in the transverse directions relies more heavily on the E_2 found from strand tests to have a high level of variation. In addition, transverse E may depend more heavily on horizontal density variations created during forming, thus invalidating the ROM assumption of having uniform horizontal density profile. The deformation and failure was observed to occur at low density areas that are not characterized by the high density strand properties used in transformation.

Strand Length (cm)		30	20	30	30	20	20	10	10
Stand Width (cm)		1.25	all	1.9	2.5	all	all	all	All
Vane Spacing (cm)		7.6	3.8	7.6	7.6	3.8	7.6	3.8	7.6
Tensor Transformation	Normal	-37.5		-166.0	-193.2		-77.4		-78.4
	Weibull	-39.1		-184.5	-205.7		-82.0		-79.5
	Mean	-28.7		-141.6	-170.0		-52.1		-21.2
Hankinson	Normal	-34.0		-156.6	-186.8		-70.5		-67.0
	Weibull	-34.8		-173.1	-196.8		-74.1		-67.6
	Mean	**-26.2**		**-137.5**	**-167.3**		**-49.2**		**-15.9**

Table 11: *Percent Error predicted to measured tensile transverse E using multiple methods*

Comparison of Design Models

Barnes' model using the measured mean strand angle predicted parallel properties more accurately, on average, than tensor transformation with ROM. However, Barnes' model was less accurate if predictions were made with the predicted mean angle. This is illustrated by the high percent COV for the percent errors of Barnes' model (**Table 12**). Modification of properties using tensor transformation was consistent across all of the tested strand geometries, shown by the much low percent COV. Tensor transformation of angular distributions using the ROM are a more accurate method of predicting parallel elastic properties than mean strand angle and the Hankinson equation with an *n* of 2. The normal distribution, with easily estimated parameters appears to predict more accurately than the 2-parameter Weibull. Unfortunately numerical integration is needed to find probabilities. This is easily accomplished using computer software.

Average % Error (%COV)	Barnes predicted $\bar{\theta}$	Barnes measured $\bar{\theta}$	Hankinson $\bar{\theta}$	Hankinson normal distribution	Tensor $\bar{\theta}$	Tensor normal distribution
Parallel	29.3 (121)	14.0 (70.8)	43.2 (28.4)	20.8 (20.6)	35.9 (36.1)	15.7 (28.2)
Transverse	X	X	79.2 (86.7)	103.0 (63.3)	82.7 (82.7)	110.5 (59.6)

Table 12: *Comparison of design procedures*

The dependence of predictions of E on standard deviation using tensor transformation is illustrated by **Figure 11**. The values used for aspen are those found with strand testing. The Loblolly pine and Yellow-poplar properties are from the Wood Handbook. The additional species were chosen because of their current application in strand composites. Transformed properties are reliant on standard deviation when using the normal distribution, but also on the relationships between the principal material properties. This interaction of properties is responsible for the intersection of the lines, if the relationships were the same, the lines would be parallel.

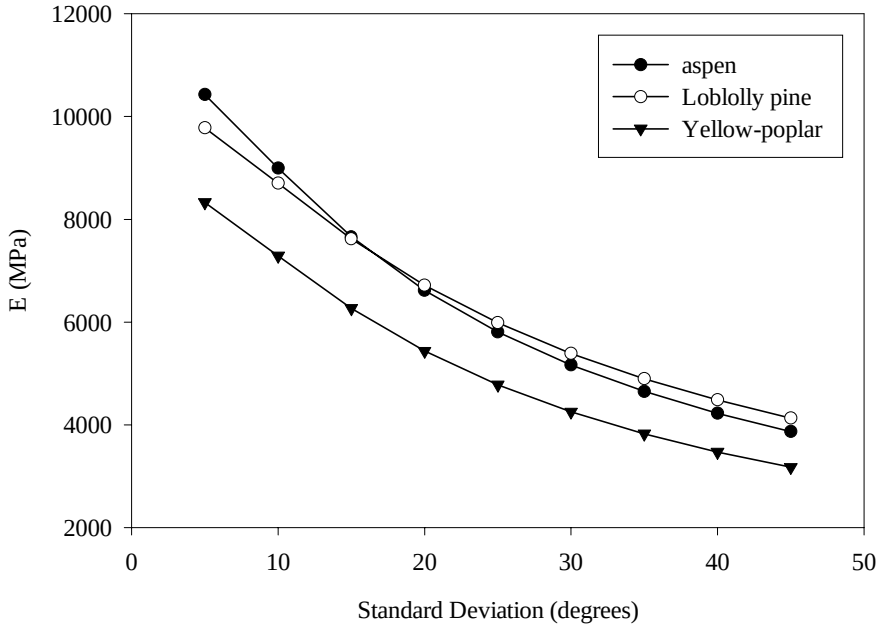

Figure 11: *Effect of standard deviation on parallel E using tensor transformation*

CONCLUSIONS

Tensor transformation of angles described by the normal distribution and implemented using the ROM predicted parallel E_c consistently well with some added computational difficulty over the entire range of strand geometries tested. This method is well suited for products that do not fall into the range defined by Barnes. This is especially important for research involving new products. In addition, transverse E_c can be determined without having to define empirical relationships needed to utilize Barnes' model. However, the semi-empirical method works well on average with a measured mean strand angle and can be done quickly and without difficulty within the range of variable used to define the empirical factors.

REFERENCES

Barnes, Derek. *An Integrated Model of the Effect of Processing Parameters on the Strength Properties of Oriented Strand Wood Composites*. Forest Products Journal. 50(11/12), 2000. pp. 33-42.

Bodig, Jozsef and James R. Goodman. *Prediction of Elastic Parameters for Wood*. Wood Science. 5(4), 1973. pp. 249-264.

Harris, Robert A. and Jay A. Johnson. *Characterization of Flake Orientation in Flakeboard by the von Mises Probability Distribution Function*. Wood and Fiber. 14(4), 1982. pp. 254-266.

Hoover, William L., Michael O. Hunt, Robert C. Lattanzi, James H. Bateman, John A. Youngquist. *Modeling Mechanical Properties of Single-Layer, Aligned, Mixed-Hardwood Strand Panels*. Forest Products Journal. 42(5). 1992. pp. 12-18.

Kellogg, Robert M. and Geza Ifju. *Influence of Specific Gravity and Certain Other Factors on the Tensile Properties of Wood*. Forest Products Journal. October 1962. pp. 463-470.

Kettogoda, Nathabandu T. and Renzo Rosso. Statistics, Probability, and Reliability for Civil and Environmental Engineers. McGraw-Hill Companies, Inc. New York. 1997. Pp. 214 and 218-219.

Meyers, Kristin. *Modeling of oriented strand composites based on strand geometry and orientation for single layer panels: Appendix*. Master's Thesis. Washington State University. 2001a.

Meyers, Kristin. *Modeling of oriented strand composites based on strand geometry and orientation for single layer panels: Chapter 2*. Master's Thesis. Washington State University. 2001b.

Palka, L.C. *Predicting the Effect of Specific Gravity, Moisture Content, Temperature and Strain Rate on the Elastic Properties of Softwoods.* Wood Science and Technology. Vol. 7. 1973. pp. 127-141.

Shaler, S.M. *Comparing Two Measures of Flake Alignment*. Wood Science and Technology. 26, 1991. pp. 53-61.

Triche, Michael H., and Hunt, Michael O. *Modeling of Parallel-Aligned Wood Strand Composites.* Forest Products Journal. Vol. 43 #11/12 1993. pp. 33-44.

Wang, Kaiyuan and Lam, Frank . *Quadratic RSM Models of Processing Parameters for Three-layer Oriented Flakeboard.* Wood and Fiber Science. April 1999, 31(2). pp. 173-186.

Wood Handbook #72 1987.U.S. Forest Products Laboratory, pp 4-14, 4-25, 4-29.

Xu, Wei and Suchsland, Otto. *Modulus of Elasticity of Wood Composite Panels with a Uniform Vertical Density Profile: A Model*. Wood and Fiber Science. 30(3), 1998. pp. 293-300.

CHAPTER 4

SUMMARY AND CONCLUSIONS

Strand geometry, within the range used in this study, does not significantly influence oriented strand composite properties when strand orientation is considered. While both strand orientation and specimen density do influence properties. Increasing orientation increased parallel properties and decreases transverse values. Increasing density increases properties in both panel directions. Strand geometry does not directly control panel properties for the range of geometries considered. However, it does play a role in orienting strands with a mechanical orienter and the range does span the geometries used in both commercial OSB and OSL. Panels can be manufactured with shorter strands and achieve properties needed for the applications currently reserved for oriented strand lumber (OSL) manufactured with 30 cm strands, if a method of attaining adequate levels of orientation can be developed. Utilization of shorter strands would allow existing oriented strand board (OSB) plants to be inexpensively converted to (OSL) plants, which turn out a higher value commercial product.

Semi-empirical and more fundamentally based models for parallel elastic properties were evaluated. Transverse properties were not predicted well by using tensor transformation. Barnes' model, with multiple fully empirical relationships was not applied to the transverse direction. However, the best predictions were made using the Hankinson equation with the general exponent and a mean angle. All methods over predicted the values obtained from testing. The higher percent error may be a result of assumptions involved with determining the model inputs obtained from flake testing will influence the model outputs. In addition, columns of low and high density material were occurred during forming creating a non-uniform horizontal density profile which violates the assumptions of the parallel rule of mixtures.

Another possible source of error is the out of plane angle in the transverse direction is visually much greater than the parallel direction. The assumption that the out of plane angle is negligible may not be valid for this direction.

Parallel properties were predicted well using both the semi-empirical methods and the fundamental approach. Barnes' model predicted the parallel elastic modulus (E) well if the measured mean strand angle was used. Transverse properties can not be predicted using Barnes' model because all of the empirical relationships were fit to parallel property data. Use of the Hankinson equation with either mean angle or a distribution of angles and the ROM with an empirical exponent of 2.0 did not predict parallel E well. Tensor transformation and the ROM following a distribution of angles, however, predicted parallel properties consistently well for all strand lengths considered. Predictions of properties outside of the current panel strand geometries is possible without the empirical reliance on data, allowing for innovation in strand composites.

APPENDIX

APPENDIX A: PRESS CYCLE

The following is the press schedule used in pressing all panels.

PressMAN v7.8 Press Control rel. 06/14/2000 SK Software Copyright 1990-2000

Proj. Ref.: Kristin Meyers	Date.....: 02-09-2001	Time.....: 12:55:07
Prod. Ref.: 360F	Panel ID..: km360-4	File Name.: KM360.REG
Press ID..: WSUWW	Mat Length: 1.37 m	Mat Width.: 1.17 m
Density...: 593 kg/m3	Thickness.: 18.54 mm	Caul Thick: 5.08 mm
Units.....: METRIC	Pressure..: MAT	Position..: THICKNESS

SEGMENT	CONTROL	SETPOINT	SEG. TIME	END CONDITION	EVENTS
1	FASTPOSN	-50.80 mm/s	25 s	POSITION <= 152.40 mm	1
2	POSITION	50.00%	1 s		2
3	POSITION	50.00%	5 s		2
4	POSITION	114.30 mm	20 s		
5	POSITION	63.50 mm	20 s		
6	POSITION	18.54 mm	20 s		
7	POSITION	18.54 mm	620 s		
8	POSITION	20.32 mm	120 s		
9	POSITION	21.59 mm	60 s		
10	FASTPOSN	50.80 mm/s	90 s	POSITION >= 811.05 mm	1

EVENT Listing:

EVENT 1: Fast Position Control	EVENT 2: Not Used
EVENT 3: Follow Density Rate Profile	EVENT 4: Not Used
EVENT 5: Begin Steam Injection Program	EVENT 6: Run Steam Injection Program
EVENT 7: Not Used	EVENT 8: Not Used
EVENT 9: Decelerate from Set Rate to 0	EVENT 10: Accelerate from 0 to Set Rate
EVENT 11: Setpoint is Given as Rate	EVENT 12: PID Control is Manual

PRESS PRESSURE/ POSITION	LOOP 1	LOOP 2	LOOP 3
PID parameter	Pressure	Position	Fast Position
Gain	1.20%	50.00%	1.00%
Reset	0.10%	2.00%	0.10%
Rate	0.00%	0.00%	0.00%
Bias	50.00%	50.00%	50.00%
Dead Band	0.00%	0.00%	0.00%

The following is graph showing internal gas pressure, core temperature, mat pressure and position throughout the press cycle. This information was obtained during the manufacture of a practice panel.

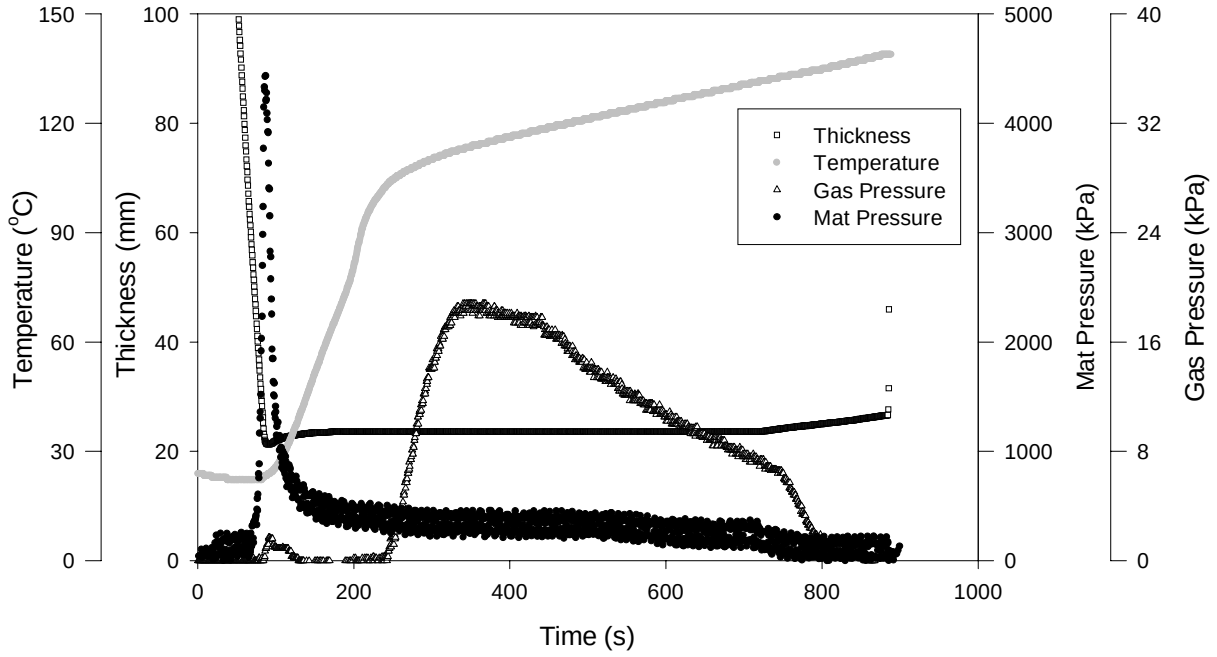

Figure A.12: *Probe output of press schedule*

APPENDIX B: NON-DESTRUCTIVE TESTING

Non-destructive testing of panels was done using stress-wave timing. Propagation time of the wave was recorded to find the wave speed (time/length). This speed is related to the panel rigidity through Equation 1A (Tucker 2001).

$$Q_{ii} = C_{ph}^2 \cdot \rho = \frac{E_i}{(1 - \nu_{12}\nu_{21})} \qquad \text{Equation 1A}$$

Where, C_{ph} is the stress wave velocity (m/s) found by dividing the distance the wave traveled by the arrival time (defined as the time when the 1st noticeable variation from the zero axis on the fluke) (Tucker 2001), ρ is the panel density (kg/m3), Q is the panel rigidity (Pa), E is the panel elasticity (Pa), ν_{12} and ν_{21} are Possion's ratios.

Values of are ν_{12} and ν_{21} on the order of 0.3 and 0.05 respectively (Wood Handbook). The product of these values is small in comparison to one and can be neglected leaving E approximately equal to Q. This allowed the calculation of dynamic E_1 and E_2, the parallel and transverse E, respectively (**Table A.13**).

Strand Length (cm)	Strand Width (cm)	Vane Spacing (cm)	NDE E1 (MPa)	E1 measured (MPa)	NDE to measured (E1)	NDE E2 (MPa)	E2 measured (MPa)	NDE to measured (E2)
30	1.25	7.6	18662	12002	1.55	1533	638	2.40
30	1.9	7.6	18938	11812	1.60	1518	444	3.42
30	2.5	7.6	20466	12964	1.58	1420	426	3.33
20	1.25	3.8	19872	13646	1.46	1250	366	3.41
20	1.9	3.8	20229	12722	1.59	1228	318	3.87
20	2.5	3.8	19887	13729	1.45	1348	415	3.25
20	1.25	7.6	16960	13226	1.28	1551	973	1.59
20	1.9	7.6	18180	12461	1.46	1594	703	2.27
20	2.5	7.6	18538	12818	1.45	1797	1080	1.66
10	1.25	3.8	18175	11944	1.52	1609	528	3.05
10	1.9	3.8	17949	12843	1.40	1622	496	3.27
10	2.5	3.8	19081	12433	1.53	1602	522	3.07
10	1.25	7.6	13543	7918	1.71	3575	1112	3.22
10	1.9	7.6	13719	9345	1.47	2884	1142	2.53
10	2.5	7.6	14349	9333	1.54	3029	946	3.20

Table A.13: *Elastic moduli predicted using stress-wave timing compared to tensile values*

The values of E predicted for both the parallel and transverse directions consistently overpredicted the measured values. This is partly a result of ignoring the effect of the Possion's ratios. Also, the NDE modulus is dynamic and the measured E from testing is static.

References

Tucker, Brian J. 2001. *Ultrasonic Plate Waves in Wood-Based Composite Panels*. Ph.D. Dissertation. Washington State University.

APPENDIX C: COMPARISON OF DISTRIBUTIONS

The literature expresses the importance of orientation on strand composite properties. Most researchers rely on a mean angle. To increase accuracy in describing the angular data for each panel distributions were fit. The two distributions that had the most desirable traits and fit well are the 2-parameter Weibull and the normal distribution. These are not the only distributions considered. This appendix explains why these distributions were chosen.

The von Mises distribution has been used to describe angular data of strand board (Shaler 1991 and Harris & Johnson 1982). This distribution was developed for angular data between +/- π or +/- $\pi/2$. The integral of the probability density function (pdf) does not have a closed form solution and will have to be numerically integrated. The von Mises pdf with an assumed mean of 0 is defined by Equation 2A.

$$p(\theta;0,\kappa)=\frac{1}{\pi I_o(\kappa)}e^{\kappa\cos\theta} \qquad for \ -\pi/2 \le \theta \le \pi/2 \qquad \text{Equation 2A}$$

Where: θ = strand angle (radians), κ = concentration parameter (constant for a given distribution) and $I_o(\kappa)$ = modified Bessel function of order 0 evaluated at κ (constant)

The parameters of the von Mises distribution were fit using Mathematica software. The frequency distribution of the angles was set equal to the von Mises pdf. A nonlinear fit function iterated until the sums of squares were minimized and the parameters were determined. This distribution did not fit the data well. The dependence on a single parameter did not allow for changing both shape and scale to match the frequency distribution. An example of this is shown in **Figure A.13**.

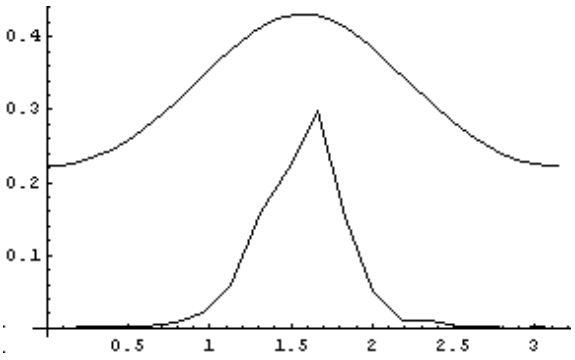

Figure A.13: *Example of the fit of the von Mises distribution*

The beta distribution was also considered and has two parameters and a versatile shape, but lacks a closed form solution to the pdf defined by Equation 3A (Law and Kelton 1982). This distribution was also evaluated for the data by minimizing sums of squares to find the best fit parameters. The angular data had to be normalized to values of 0 to 1. In addition, for low peak values, the distribution has more probability in the tails. The data's frequency distribution is not skewed, but had peak values around 0.2, with minimal tails. This distribution did not provide a good fit (**Figure A.14**).

$$p(\theta;\alpha,\beta) = \frac{1}{B(\alpha,\beta)}\theta^{\alpha-1}(1-\theta)^{\beta-1} \qquad for \;\; 0<\theta<1, \alpha>0, \beta>0$$ Equation 3A

Where θ = random variable (strand angle), α = shape parameter, β = shape parameter, B(α,β) = beta function

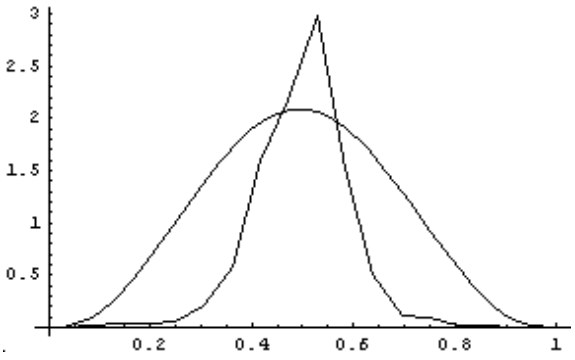

Figure A.14: *Example of fit of the Beta distribution*

The 2-parameter Weibull has a closed form solution and is defined by 2 parameters that are easily estimated using computer software. One parameter defines the distribution's shape and the other accounts for the scale. The closed form solution to the pdf is shown in Equation 4A as the cumulative distribution function (CDF) (Law and Kelton 1982). All values of the random variable have to be greater than 0. The Cramer-von Mises, Anderson-Darling and Chi-Square goodness of fit statistics show this distribution fits through significant p-values. This means that the null hypothesis, that the data is not described by the 2-paramter Weibull, is rejected. An example of fit is shown in **Figure A.15**.

$$CDF = \begin{matrix} 1 - e^{-(\theta/\beta)^{\alpha}} & if\ \theta > 0 \\ 0 & if\ \theta \le 0 \end{matrix} \qquad \text{Equation 4A}$$

Where: α is the shape parameter, β is the scale parameter and θ is the random variable (strand angle)

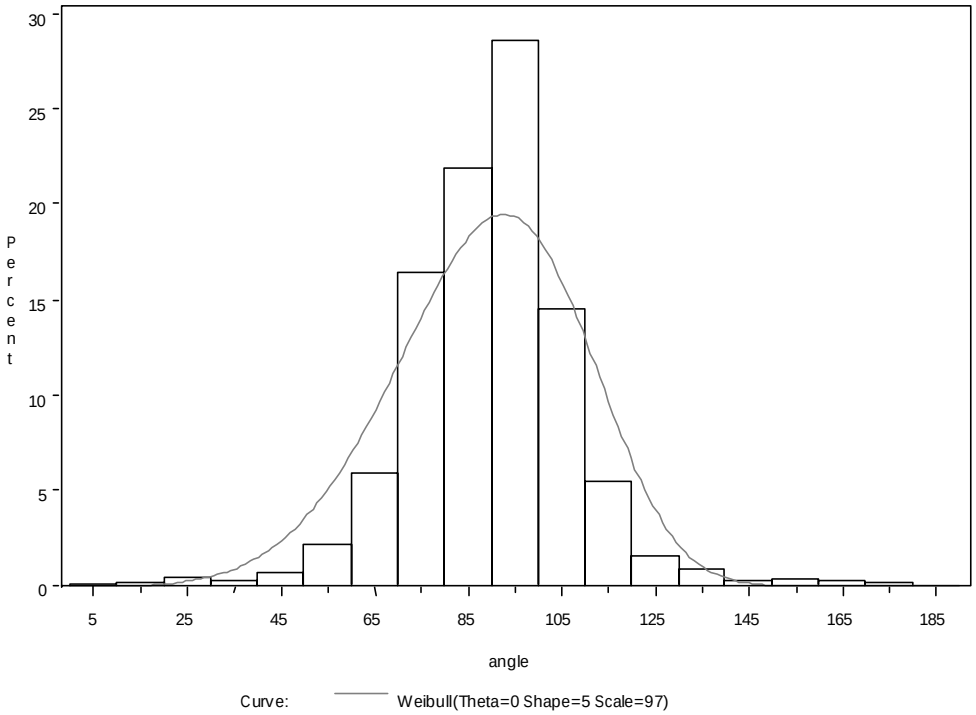

Figure A.15: *Example of the fit of the 2-parameter Weibull distribution*

The normal distribution was also fit. The parameters, mean and standard deviation, of this distribution as simple to obtain. However, the pdf (Equation 5A) has no closed form solution and will therefore have to be numerically integrated (Law and Kelton 1982). The p-values for the goodness of fit tests show that this distribution fit the data well (**Figure A.16**).

$$p(\theta;\mu,\sigma) = \frac{1}{\sqrt{2\pi\sigma^2}} e^{-(\theta-\mu)^2/2\sigma^2} \qquad \textit{for all real}\ \theta$$ Equation 5A

Where: θ is the random variable (strand angle), μ is the mean and σ is the standard deviation.

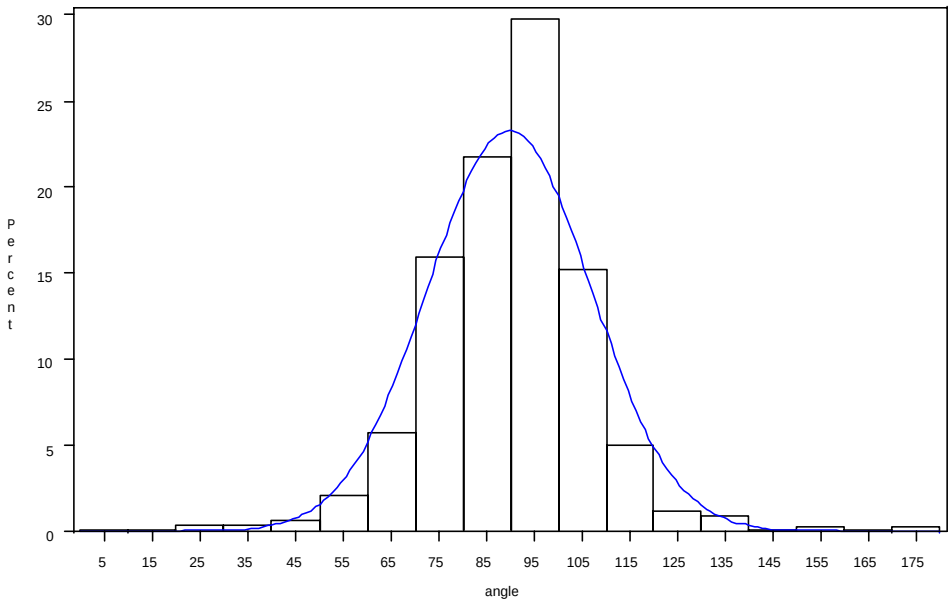

Figure A.16: *Example of the fit of the normal distribution*

APPENDIX D: ASSUMPTION OF ORTHOTROPIC PANEL BEHAVIOR

The assumption that the flake's principal material direction coincides with the long axis of the flake is not always true. If this is the case, the assumption that the composite material is orthotropic is violated. The material would in reality be generally anisotropic. In a 2-dimenstional generally anisotropic compliance matrix, S, the S_{16} and S_{26} terms are not zero, as in the orthotropic compliance matrix. Unlike the other terms in the compliance matrix, there is no relationship between material properties that define these terms, therefore each term has to be determined experimentally. The tension, compression and internal bond tests performed do not provide data that can define these terms. Therefore, the S_{16} and S_{26} terms are assumed to be zero.

The validity of this assumption is evaluated in this appendix. The average angle of grain within a sample of 46 strands was determined using laser scanning technology at the Alberta Research Council. This angle is 2.84 degrees. Material properties were taken from the Wood Handbook for E_1, E_2, G_{12}, and ν_{12}. These properties were altered using tensor transformation to find the transformed compliance matrix, S-bar. The S-bar matrix was then transformed for four different mean angles found in a composite: 12, 15, 18, and 20 degrees. This was done in two ways.

First, the full, generally anisotropic, S-bar matrix was transformed. The new S-bar 11 and 22 terms were inverted to find E_x and E_y. The values found from this procedure are the values that are obtained if the grain in the strand is not assumed to coincide with the long axis of the strand. In contrast to this, the first S-bar matrix was transformed with the 12 and 16 terms assumed to be zero. The 11 and 12 terms in the new S-bar matrix were then inverted to find the

E_x and E_y terms for the case where the flake grain and length are the same. **Table A.14** summarizes the results.

Angle (degrees)	Real E_y (MPa)	Real E_x (MPa)	Assume E_y (MPa)	Assume E_x (MPa)	Real/Assume	
12	6455	929	7370	909	0.876	1.022
15	5490	958	6314	933	0.869	1.027
18	4675	994	5383	963	0.868	1.033
20	4211	1022	4841	985	0.870	1.038

Table A.14: *Comparison of E values with and without simplifying assumption*

Transformation performed with $Sbar_{16}$ and $Sbar_{26}$ equal to zero consistently over predicted E_y by around 14%. E_x was under predicted by 2-4%. The error of the parallel composite E, E_y, is large. The error found above is a worst case scenario for the grain angle used. The calculations assumed that the angle of grain in a strand would always add to the off-axis angles of the strand. This would not always be true. It is just as likely that the off-axis angle would be reduced by the angle of grain.

APPENDIX E: TRANSFORMATION OF THE COMPLIANCE MATRIX

This appendix outlines the steps taken to transform the compliance matrix, S, a 4th order tensor. Equation 6A relates the principal stress and principle tensor strain through the compliance matrix, S. The transformation matrix is defined using tensor strain.

$$\begin{bmatrix} \varepsilon_1 \\ \varepsilon_2 \\ \gamma_{12} \end{bmatrix} = [S] \cdot \begin{bmatrix} \sigma_1 \\ \sigma_2 \\ \tau_{12} \end{bmatrix} \qquad \text{Equation 6A}$$

Test results are stress and engineering strain. Engineering strain is related to tensor strain by using the Reuter matrix as shown in Equation 7A.

$$\begin{bmatrix} \varepsilon_1 \\ \varepsilon_2 \\ \gamma_{12} \end{bmatrix} = \begin{bmatrix} 1 & 0 & 0 \\ 0 & 1 & 0 \\ 0 & 0 & 2 \end{bmatrix} \cdot \begin{bmatrix} \varepsilon_1 \\ \varepsilon_2 \\ \gamma_{12}/2 \end{bmatrix} \qquad \text{Equation 7A}$$

Transformation is used to find material properties, stresses or strains at an orientation other than the principle material axes. This off-axis orientation will be referred to as the x-y coordinate system. To transform the strain from the 1-2 coordinate system to the x-y coordinate system Equation 8A is used.

$$\begin{bmatrix} \varepsilon_x \\ \varepsilon_y \\ \gamma_{xy} \end{bmatrix} = [R][T]^{-1}[R]^{-1} \begin{bmatrix} \varepsilon_1 \\ \varepsilon_2 \\ \gamma_{12} \end{bmatrix} \qquad \text{Equation 8A}$$

Now, from equation 1D $[S][\sigma_{12}]$ replaces $[\varepsilon_{12}]$. To get stress in the x-y coordinate system, $[\sigma_{12}]$ is replaced with $[T]\,[\sigma_{xy}]$. This yields Equation 9A.

$$\begin{bmatrix} \varepsilon_x \\ \varepsilon_y \\ \gamma_{xy} \end{bmatrix} = [R][T]^{-1}[R]^{-1}[S][T] \begin{bmatrix} \sigma_x \\ \sigma_y \\ \tau_{xy} \end{bmatrix} \qquad \text{Equation 9A}$$

This can be reduced by noting that $[R][T]^{-1}[R]^{-1}$ is equal to $[T]^{T}$ as shown in Equation 10A.

$$\begin{bmatrix} \varepsilon_x \\ \varepsilon_y \\ \gamma_{xy} \end{bmatrix} = [T]^T [S][T] \begin{bmatrix} \sigma_x \\ \sigma_y \\ \tau_{xy} \end{bmatrix} \qquad \text{Equation 10A}$$

The factor that relates strain in the x-y system to stress in the x-y system is the transformed compliance matrix, shown in Equation 11A.

$$\left[\bar{S}\right] = [T]^T [S][T] \qquad \text{Equation 11A}$$

APPENDIX F: COMPRESSION DATA AND STATISTICAL ANALYSES

Compression parallel data

This analysis was run on the parallel compression data to identify factors were significant in a model for parallel compression E and strength. Also included are the mean, standard deviation, min and max for each length, width and vane spacing combination after the strength data. These statistics are provided for E, density, mean angle, strength. Density and angle are significant factors in the model, but length and width are not.

Comparison of all Parallel Compression Data

The GLM Procedure
Class Level Information

Class	Levels	Values
length	3	4 8 12
width	3	0.5 0.75 1
vane	2	1.5 3

Number of observations 130

Dependent Variable: E

Source	DF	Sum of Squares	Mean Square	F Value	Pr > F
Model	6	8.706421E12	1.4510702E12	24.55	**<.0001**
Error	123	7.2696797E12	59103087149		
Corrected Total	129	1.5976101E13			

R-Square	Coeff Var	Root MSE	E Mean
0.544965	21.85217	243111.3	1112527

Source	DF	Type III SS	Mean Square	F Value	Pr > F
length	2	74571272236	37285636118	0.63	0.5338
width	2	214806022381	107403011191	1.82	0.1668
density	1	3.6133003E12	3.6133003E12	61.14	**<.0001**
angle	1	2.430155E12	2.430155E12	41.12	**<.0001**

Dependent Variable: strength

Source	DF	Sum of Squares	Mean Square	F Value	Pr > F
Model	6	82248809.0	13708134.8	84.69	**<.0001**
Error	123	19910032.3	161870.2		
Corrected Total	129	102158841.3			

R-Square	Coeff Var	Root MSE	strength Mean
0.805107	11.26093	402.3309	3572.805

Source	DF	Type III SS	Mean Square	F Value	Pr > F
length	2	129294.02	64647.01	0.40	0.6716
width	2	193832.31	96916.15	0.60	0.5511
density	1	46019959.80	46019959.80	284.30	**<.0001**
angle	1	14260987.15	14260987.15	88.10	**<.0001**

---------- length=12 width=0.5 vane=3 ----------

Variable	N	Mean	Std Dev	Minimum	Maximum
angle	7	18.4285714	0.9759001	17.0000000	19.0000000
density	7	40.4780219	3.5341002	33.7213826	44.6528667
strength	7	4008.02	530.3242922	3022.49	4707.71
E	7	1101694.29	303815.74	748349.00	1583020.00

---------- length=12 width=0.75 vane=3 ----------

Variable	N	Mean	Std Dev	Minimum	Maximum
angle	9	17.0000000	1.5000000	16.0000000	19.0000000
density	9	42.1341066	5.0966392	36.3973265	52.5580311
strength	9	3962.01	829.3894642	2423.66	5487.97
E	9	1239639.67	369445.51	881099.00	1833590.00

---------- length=12 width=1 vane=3 ----------

Variable	N	Mean	Std Dev	Minimum	Maximum
angle	8	14.2500000	0.4629100	14.0000000	15.0000000
density	8	38.7435681	4.4518267	32.9083965	47.2217317
strength	8	3960.70	871.9601629	3076.02	5838.73
E	8	1307421.25	247962.39	1101470.00	1897610.00

---------- length=4 width=0.5 vane=3 ----------

Variable	N	Mean	Std Dev	Minimum	Maximum
angle	9	28.6666667	1.8027756	27.0000000	31.0000000
density	9	39.9612232	5.6906333	33.2069060	49.7158101
strength	9	2880.03	594.1004005	1866.81	3942.34
E	9	818291.56	175196.28	570634.00	1092470.00

---------- length=4 width=0.5 vane=1.5 ----------

Variable	N	Mean	Std Dev	Minimum	Maximum
angle	9	18.0000000	0.8660254	17.0000000	19.0000000
density	9	38.2962182	2.1658695	33.6786769	40.9926354
strength	9	3629.86	497.6005994	3041.79	4404.82
E	9	1160471.78	232393.00	779220.00	1423420.00

---------- length=4 width=0.75 vane=3 ----------

Variable	N	Mean	Std Dev	Minimum	Maximum
angle	9	28.6666667	1.0000000	28.0000000	30.0000000
density	9	36.2220051	3.5164296	31.5896578	42.6919866
strength	9	2619.60	526.4469059	1915.44	3328.70
E	9	735561.90	311507.47	1.0745700	1016600.00

------------------------ length=4 width=0.75 vane=1.5 ------------------------

Variable	N	Mean	Std Dev	Minimum	Maximum
angle	9	19.3333333	1.3228757	18.0000000	21.0000000
density	9	35.9201330	4.9869117	29.2451671	44.9999479
strength	9	3152.50	1006.17	1425.99	4509.78
E	9	961188.56	229015.68	549054.00	1299900.00

--------------------------- length=4 width=1 vane=3 ---------------------------

Variable	N	Mean	Std Dev	Minimum	Maximum
angle	9	28.3333333	1.3228757	27.0000000	30.0000000
density	9	35.8816842	2.8631308	31.8421520	41.8283440
strength	9	2426.07	345.4442345	1934.43	3007.24
E	9	700869.11	204197.01	412266.00	995906.00

------------------------- length=4 width=1 vane=1.5 --------------------------

Variable	N	Mean	Std Dev	Minimum	Maximum
angle	9	17.6666667	0.5000000	17.0000000	18.0000000
density	9	39.6616837	4.4038623	33.8487992	47.2756098
strength	9	3861.09	577.9996458	3288.15	4894.07
E	9	1317273.89	425294.25	831694.00	2165810.00

------------------------- length=8 width=0.5 vane=3 --------------------------

Variable	N	Mean	Std Dev	Minimum	Maximum
angle	9	19.0000000	0.8660254	18.0000000	20.0000000
density	9	39.4425686	3.6219208	34.6699760	43.8852705
strength	9	3649.05	792.1733081	2636.58	4713.72
E	9	1170179.00	339097.80	657825.00	1585430.00

------------------------- length=8 width=0.5 vane=1.5 -------------------------

Variable	N	Mean	Std Dev	Minimum	Maximum
angle	9	12.0000000	0	12.0000000	12.0000000
density	9	40.0063939	4.3046194	32.1666198	45.7026997
strength	9	4366.50	883.1602439	2919.93	5636.45
E	9	1311422.67	347750.97	791216.00	1873650.00

------------------------- length=8 width=0.75 vane=3 -------------------------

Variable	N	Mean	Std Dev	Minimum	Maximum
angle	8	17.7500000	1.0350983	17.0000000	19.0000000
density	8	40.3581227	4.5628840	31.6780531	45.6055763
strength	8	3668.91	1164.31	1522.84	4962.15
E	8	1195156.25	258655.31	747512.00	1525380.00

------------------------ length=8 width=0.75 vane=1.5 ------------------------

Variable	N	Mean	Std Dev	Minimum	Maximum
angle	8	12.6250000	1.4078860	11.0000000	14.0000000
density	8	35.6938141	3.5107535	31.0643702	40.2645194
strength	8	3737.57	680.2722155	2766.30	4819.18
E	8	1147202.00	315253.25	821692.00	1709160.00

```
--------------------------- length=8 width=1 vane=3 ----------------------------
Variable      N            Mean         Std Dev         Minimum         Maximum
ffffffffffffffffffffffffffffffffffffffffffffffffffffffffffffffffffffffffffffff
angle         9      18.3333333       0.5000000      18.0000000      19.0000000
density       9      38.5166243       4.6693084      31.6284210      46.0065283
strength      9         3565.37     675.6038155         2535.47         4478.67
E             9      1127157.56       281595.00       737650.00      1442040.00
ffffffffffffffffffffffffffffffffffffffffffffffffffffffffffffffffffffffffffffff
--------------------------- length=8 width=1 vane=1.5 --------------------------
Variable      N            Mean         Std Dev         Minimum         Maximum
ffffffffffffffffffffffffffffffffffffffffffffffffffffffffffffffffffffffffffffff
angle         9      13.6666667       0.5000000      13.0000000      14.0000000
density       9      38.9654527       3.9862037      31.4008548      45.1658232
strength      9         4273.60     528.2634321         3425.29         5142.68
E             9       1426651.67       269843.59        913295.00       1651740.00
```

Compression transverse data

This analysis was run on the transverse compression data to identify factors were significant in a model for parallel compression E and strength. Also included are the mean, standard deviation, min and max for each length, width and vane spacing combination after the strength data. These statistics are provided for E, density, mean angle, strength. Density and angle are significant factors in the model for E, but length and width are not. Density, mean angle and length were all significant for strength. The 4 inch strands are different from the 8 and 12 inch strands.

```
Comparison of all Perpendicular Compression Data

                            The GLM Procedure
                         Class Level Information

                    Class         Levels    Values
                    length             3    4 8 12
                    width              3    0.5 0.75 1
                    vane               2    1.5 3
                       Number of observations    109
Dependent Variable: E
                                       Sum of
 Source                     DF        Squares    Mean Square   F Value   Pr > F
 Model                       6   164341430103    27390238351     29.19   <.0001
 Error                     102    95711937099    938352324.5
 Corrected Total           108   260053367203

               R-Square     Coeff Var      Root MSE        E Mean
               0.631953      29.51351      30632.54      103791.6
 Source                     DF    Type III SS    Mean Square   F Value   Pr > F
 length                      2     3896134235     1948067118      2.08   0.1307
```

width	2	1192029588	596014794	0.64	0.5319
density	1	29454699781	29454699781	31.39	**<.0001**
angle	1	91209550326	91209550326	97.20	**<.0001**

Dependent Variable: strength

Source	DF	Sum of Squares	Mean Square	F Value	Pr > F
Model	6	4132088.935	688681.489	88.08	**<.0001**
Error	102	797535.821	7818.979		
Corrected Total	108	4929624.756			

R-Square	Coeff Var	Root MSE	strength Mean
0.838216	10.88612	88.42499	812.2730

Source	DF	Type III SS	Mean Square	F Value	Pr > F
length	2	193891.889	96945.945	12.40	**<.0001**
width	2	27069.276	13534.638	1.73	0.1823
density	1	2501465.860	2501465.860	319.92	**<.0001**
angle	1	596097.812	596097.812	76.24	**<.0001**

Tukey's Studentized Range (HSD) Test for strength

NOTE: This test controls the Type I experimentwise error rate.

Alpha	0.05
Error Degrees of Freedom	102
Error Mean Square	7818.979
Critical Value of Studentized Range	3.36361

Comparisons significant at the 0.05 level are indicated by ***.

length Comparison	Difference Between Means	Simultaneous 95% Confidence Limits		
4 - 8	**182.33**	**136.68**	**227.99**	***
4 - 12	**234.02**	**179.97**	**288.07**	***
8 - 4	**-182.33**	**-227.99**	**-136.68**	***
8 - 12	51.69	-1.68	105.05	
12 - 4	**-234.02**	**-288.07**	**-179.97**	***
12 - 8	-51.69	-105.05	1.68	

---------- length=12 width=0.5 vane=3 ----------

Variable	N	Mean	Std Dev	Minimum	Maximum
angle	7	18.4285714	0.9759001	17.0000000	19.0000000
IB	7	54.2048292	1.1317759	53.5308360	55.8614756
density	7	40.1342857	1.5158260	38.3700000	42.7400000
strength	7	677.2737143	103.8924422	544.8570000	808.7030000
E	7	85181.43	16985.55	62969.00	108049.00

---------- length=12 width=0.75 vane=3 ----------

Variable	N	Mean	Std Dev	Minimum	Maximum
angle	8	17.1250000	1.5526475	16.0000000	19.0000000
IB	8	66.6138752	7.3303542	58.3642644	75.4160230
density	8	40.8525000	3.9527414	36.5500000	48.7500000
strength	8	711.4167500	186.8481153	454.9210000	990.2610000
E	8	106268.50	41171.13	68141.00	187096.00

---------- length=12 width=1 vane=3 ----------

Variable	N	Mean	Std Dev	Minimum	Maximum
angle	9	14.3333333	0.5000000	14.0000000	15.0000000
IB	9	47.7955709	1.6210753	46.1235785	49.8178124
density	9	41.5033333	2.9138892	37.0200000	45.5400000
strength	9	716.5498889	191.4650952	427.3660000	1001.63
E	9	71871.22	30259.83	36914.00	130698.00

---------- length=8 width=0.5 vane=3 ----------

Variable	N	Mean	Std Dev	Minimum	Maximum
angle	6	19.3333333	0.8164966	18.0000000	20.0000000
IB	6	83.4453839	5.4523821	76.8249047	90.1373133
density	6	40.8266667	3.7152479	34.5100000	46.1700000
strength	6	804.9840000	166.0667874	561.3820000	1016.69
E	6	140513.17	62444.54	62075.00	245705.00

---------- length=8 width=0.5 vane=1.5 ----------

Variable	N	Mean	Std Dev	Minimum	Maximum
angle	8	12.0000000	0	12.0000000	12.0000000
IB	8	84.1219618	5.4550621	75.6039951	88.5330080
density	8	41.4862500	1.7285083	38.1300000	44.0200000
strength	8	697.9857500	140.0888553	491.5650000	874.9010000
E	8	63332.25	13016.37	48990.00	84344.00

---------- length=8 width=0.75 vane=3 ----------

Variable	N	Mean	Std Dev	Minimum	Maximum
angle	6	18.0000000	1.0954451	17.0000000	19.0000000
IB	6	70.2507874	4.0488497	67.5842920	75.4767337
density	6	42.2933333	4.2108416	38.0200000	49.7200000
strength	6	858.4946667	245.7738633	520.2930000	1243.90
E	6	128521.17	29793.53	95807.00	166151.00

---------- length=8 width=0.75 vane=1.5 ----------

Variable	N	Mean	Std Dev	Minimum	Maximum
angle	9	12.6666667	1.3228757	11.0000000	14.0000000
IB	9	75.7958287	11.1282176	63.8224418	89.3716464
density	9	40.2111111	2.2317339	37.3000000	43.8700000
strength	9	652.9683333	82.9526283	542.1090000	796.5940000
E	9	64392.89	16384.32	37487.00	88981.00

---------- length=8 width=1 vane=3 ----------

Variable	N	Mean	Std Dev	Minimum	Maximum
angle	7	18.4285714	0.5345225	18.0000000	19.0000000
IB	7	73.7531049	1.9568872	71.6809671	75.8778856
density	7	41.0614286	3.9064879	37.1400000	47.1700000
strength	7	855.4370000	220.5200272	601.7140000	1095.61
E	7	100613.14	33356.89	64611.00	161946.00

---------- length=8 width=1 vane=1.5 ----------

Variable	N	Mean	Std Dev	Minimum	Maximum
angle	8	13.6250000	0.5175492	13.0000000	14.0000000
IB	8	72.8185848	20.3357573	57.5903450	97.3728708
density	8	38.7662500	4.8502193	28.4600000	45.9300000
strength	8	724.1855000	230.3272989	244.4650000	1075.92
E	8	63405.25	25131.19	25465.00	102122.00

---------- length=4 width=0.5 vane=3 ----------

Variable	N	Mean	Std Dev	Minimum	Maximum
angle	5	28.6000000	2.1908902	27.0000000	31.0000000
IB	5	79.0476627	1.5101983	77.9447699	80.7020021
density	5	40.3540000	1.5442409	37.9200000	42.0800000
strength	5	1047.48	181.3097544	842.6070000	1280.19
E	5	186123.60	66468.60	82836.00	267026.00

---------- length=4 width=0.5 vane=1.5 ----------

Variable	N	Mean	Std Dev	Minimum	Maximum
angle	7	17.8571429	0.8997354	17.0000000	19.0000000
IB	7	84.8350694	10.6236624	70.5838038	96.2407633
density	7	39.2228571	1.4894710	37.7300000	41.0900000
strength	7	770.9522857	120.8624298	639.0210000	983.7000000
E	7	89286.71	25984.75	65425.00	137702.00

---------- length=4 width=0.75 vane=3 ----------

Variable	N	Mean	Std Dev	Minimum	Maximum
angle	6	28.6666667	1.0327956	28.0000000	30.0000000
IB	6	82.3680605	3.7685928	74.7818139	84.3952241
density	6	41.5600000	2.4357340	37.9200000	44.3500000
strength	6	1141.76	237.0035410	831.9290000	1457.04
E	6	169447.17	36669.33	105355.00	205376.00

---------- length=4 width=0.75 vane=1.5 ----------

Variable	N	Mean	Std Dev	Minimum	Maximum
angle	7	19.4285714	1.5118579	18.0000000	21.0000000
IB	7	82.5088829	9.3932970	74.8251559	92.5480273
density	7	43.3757143	2.5712309	40.1000000	48.3600000
strength	7	1016.29	182.7706954	807.5710000	1371.94
E	7	112267.00	28587.60	60433.00	152062.00

---------- length=4 width=1 vane=3 ----------

Variable	N	Mean	Std Dev	Minimum	Maximum
angle	8	28.1250000	1.2464235	27.0000000	30.0000000
IB	8	62.7185328	14.2511426	45.5290203	74.0369230
density	8	38.3050000	2.6066673	33.8400000	42.5800000
strength	8	910.3822500	141.8422412	743.4940000	1176.30
E	8	154545.25	47812.78	82638.00	227130.00

---------- length=4 width=1 vane=1.5 ----------

Variable	N	Mean	Std Dev	Minimum	Maximum
angle	8	17.7500000	0.4629100	17.0000000	18.0000000
IB	8	85.1655046	2.4450010	81.4430330	87.3095408
density	8	40.8575000	2.1048363	37.5900000	43.8300000
strength	8	818.9872500	155.5147470	579.6840000	1004.68
E	8	89193.75	23237.61	61410.00	132214.00

APPENDIX G: TENSION DATA AND STATISTICAL ANALYSES

Tension parallel data

This analysis was run on the parallel tension data to find which factors were significant in a model for parallel tensile E. Also included are the mean, standard deviation, min and max for each length, width and vane spacing combination after the strength data. These statistics are provided for E, density, mean angle, strength at failure location (failure) and strength if assumed gauge length failure occurred (gauge). Density and angle are significant factors in the model, but length and width are not.

Comparison of all Parallel Tension Data
08:54 Wednesday, October 17, 2001

The GLM Procedure

Class Level Information

Class	Levels	Values
length	3	4 8 12
width	3	0.5 0.75 1
vane	2	1.5 3

Number of observations 128

Dependent Variable: E

Source	DF	Sum of Squares	Mean Square	F Value	Pr > F
Model	6	8.0827535E12	1.3471256E12	8.32	**<.0001**
Error	121	1.9586096E13	161868562123		
Corrected Total	127	2.7668849E13			

R-Square	Coeff Var	Root MSE	E Mean
0.292125	23.18131	402328.9	1735575

Source	DF	Type III SS	Mean Square	F Value	Pr > F
density	1	1.4798614E12	1.4798614E12	9.14	**0.0030**
angle	1	3.7916902E12	3.7916902E12	23.42	**<.0001**
length	2	24710719122	12355359561	0.08	0.9266
width	2	80573856156	40286928078	0.25	0.7801

This analysis is for parallel tensile strength. The fist run is with strength calculated at the location of failure. This includes all of the grip failures that had stresses caused by more than pure tension. Tukey's comparison test found that the 4 inch strands are different from the 8 and

12 inch strands. This analysis found length and density all significant. Means based on panel type follow the GLM.

Comparison of all Parallel Tension Data

The GLM Procedure

Class Level Information

Class	Levels	Values
length	3	4 8 12
width	3	0.5 0.75 1
vane	2	1.5 3

Number of observations 128

Dependent Variable: failure

Source	DF	Sum of Squares	Mean Square	F Value	Pr > F
Model	6	48121279.0	8020213.2	11.27	**<.0001**
Error	121	86090365.8	711490.6		
Corrected Total	127	134211644.7			

R-Square	Coeff Var	Root MSE	failure Mean
0.358548	19.27426	843.4990	4376.297

Source	DF	Type III SS	Mean Square	F Value	Pr > F
density	1	15389675.46	15389675.46	21.63	**<.0001**
angle	1	172427.31	172427.31	0.24	0.6234
length	2	15028812.89	7514406.44	10.56	**<.0001**
width	2	3352233.07	1676116.53	2.36	0.0992

Tukey's Studentized Range (HSD) Test for failure

NOTE: This test controls the Type I experimentwise error rate.

Alpha	0.05
Error Degrees of Freedom	121
Error Mean Square	711490.6
Critical Value of Studentized Range	3.35583

Comparisons significant at the 0.05 level are indicated by ***.

length Comparison	Difference Between Means	Simultaneous 95% Confidence Limits		
12 - 8	132.3	-344.1	608.7	
12 - 4	**1045.4**	**567.4**	**1523.4**	***
8 - 12	-132.3	-608.7	344.1	
8 - 4	**913.1**	**514.8**	**1311.5**	***
4 - 12	**-1045.4**	**-1523.4**	**-567.4**	***
4 - 8	**-913.1**	**-1311.5**	**-514.8**	***

```
------------------------- length=12 width=0.5 vane=3 -------------------------
Variable      N            Mean         Std Dev         Minimum         Maximum
ffffffffffffffffffffffffffffffffffffffffffffffffffffffffffffffffffffffffffffff
density       9      39.3069561       1.5708191      37.0274051      41.9496823
angle         9      18.3333333       1.0000000      17.0000000      19.0000000
failure       9         4930.67     847.7226846         3772.00         6469.00
guage         9         5392.33     700.4270126         4413.00         6469.00
E             9      1740760.00       438568.00      1346320.00      2689580.00
ffffffffffffffffffffffffffffffffffffffffffffffffffffffffffffffffffffffffffffff
------------------------- length=12 width=0.75 vane=3 -------------------------
Variable      N            Mean         Std Dev         Minimum         Maximum
ffffffffffffffffffffffffffffffffffffffffffffffffffffffffffffffffffffffffffffff
density       9      39.4385005       2.2045939      36.4763677      43.2661699
angle         9      17.0000000       1.5000000      16.0000000      19.0000000
failure       9         5167.00     681.4011300         4359.00         6296.00
guage         9         5278.22     637.1019890         4359.00         6296.00
E             9      1713197.78       360611.31      1387720.00      2317270.00
ffffffffffffffffffffffffffffffffffffffffffffffffffffffffffffffffffffffffffffff
-------------------------- length=12 width=1 vane=3 --------------------------
Variable      N            Mean         Std Dev         Minimum         Maximum
ffffffffffffffffffffffffffffffffffffffffffffffffffffffffffffffffffffffffffffff
density       9      38.3769848       1.7484639      36.1803856      40.7673597
angle         9      14.3333333       0.5000000      14.0000000      15.0000000
failure       9         4414.44     999.0070209         3223.00         6115.00
guage         9         5517.22     977.1731906         3539.00         6597.00
E             9      1880337.78       454595.37      1178340.00      2524700.00
ffffffffffffffffffffffffffffffffffffffffffffffffffffffffffffffffffffffffffffff
------------------------- length=8 width=0.5 vane=3 --------------------------
Variable      N            Mean         Std Dev         Minimum         Maximum
ffffffffffffffffffffffffffffffffffffffffffffffffffffffffffffffffffffffffffffff
density       9      40.7419063       1.3488221      39.0926379      42.9346174
angle         9      19.0000000       0.8660254      18.0000000      20.0000000
failure       9         5263.78         1114.81         3195.00         6169.00
guage         9         5553.44     806.1357068         3876.00         6628.00
E             9      1918217.78       612716.17      1282780.00      2961620.00
ffffffffffffffffffffffffffffffffffffffffffffffffffffffffffffffffffffffffffffff
------------------------- length=8 width=0.5 vane=1.5 -------------------------
Variable      N            Mean         Std Dev         Minimum         Maximum
ffffffffffffffffffffffffffffffffffffffffffffffffffffffffffffffffffffffffffffff
density       9      39.7876884       1.9548111      37.1261096      42.3356199
angle         9      12.0000000               0      12.0000000      12.0000000
failure       9         5064.11         1541.19         3422.00         7851.00
guage         9         6211.78         1112.15         3916.00         7851.00
E             9      1979124.44       426333.56      1307380.00      2659460.00
ffffffffffffffffffffffffffffffffffffffffffffffffffffffffffffffffffffffffffffff
------------------------- length=8 width=0.75 vane=3 -------------------------
Variable      N            Mean         Std Dev         Minimum         Maximum
ffffffffffffffffffffffffffffffffffffffffffffffffffffffffffffffffffffffffffffff
density       9      40.2383762       2.8008157      35.6570807      44.0949545
angle         9      17.6666667       1.0000000      17.0000000      19.0000000
failure       9         4874.67     992.6203957         2993.00         5865.00
guage         9         5318.22     600.3962812         4279.00         6076.00
E             9      1807336.67       473917.09      1273030.00      2528400.00
ffffffffffffffffffffffffffffffffffffffffffffffffffffffffffffffffffffffffffffff
```

---------- length=8 width=0.75 vane=1.5 ----------

Variable	N	Mean	Std Dev	Minimum	Maximum
density	8	38.8483581	1.4639286	36.1497911	40.8640138
angle	8	12.8750000	1.2464235	11.0000000	14.0000000
failure	8	4268.75	572.2868287	3560.00	5183.00
guage	8	5632.13	413.6038261	5156.00	6200.00
E	8	1845131.25	251392.72	1524480.00	2364630.00

---------- length=8 width=1 vane=3 ----------

Variable	N	Mean	Std Dev	Minimum	Maximum
density	9	41.0099047	1.4281731	38.5059685	42.7090859
angle	9	18.3333333	0.5000000	18.0000000	19.0000000
failure	9	4460.00	1133.89	3298.00	6515.00
guage	9	5708.44	607.7460636	4758.00	6515.00
E	9	1859045.56	477760.60	1213040.00	2609250.00

---------- length=8 width=1 vane=1.5 ----------

Variable	N	Mean	Std Dev	Minimum	Maximum
density	7	38.5298643	1.7854043	36.3977858	40.5494682
angle	7	13.5714286	0.5345225	13.0000000	14.0000000
failure	7	4120.86	446.3087230	3662.00	4611.00
guage	7	5343.57	510.8593600	4554.00	5942.00
E	7	1991161.43	283477.81	1383830.00	2207730.00

---------- length=4 width=0.5 vane=3 ----------

Variable	N	Mean	Std Dev	Minimum	Maximum
density	9	39.8364384	0.9113276	38.3393531	40.9612878
angle	9	28.6666667	1.8027756	27.0000000	31.0000000
failure	9	3630.33	708.6550642	2291.00	4449.00
guage	9	4101.44	518.3982810	3427.00	4726.00
E	9	1148368.33	234442.02	896546.00	1514930.00

---------- length=4 width=0.5 vane=1.5 ----------

Variable	N	Mean	Std Dev	Minimum	Maximum
density	9	39.3381407	2.5116593	35.5718812	42.3914728
angle	9	18.0000000	0.8660254	17.0000000	19.0000000
failure	9	4111.33	819.1689386	2992.00	5425.00
guage	9	5093.00	668.1435100	4113.00	5943.00
E	9	1732288.89	507966.52	1076820.00	2796830.00

---------- length=4 width=0.75 vane=3 ----------

Variable	N	Mean	Std Dev	Minimum	Maximum
density	6	39.0911608	1.0315766	37.2637580	39.8650215
angle	6	29.0000000	1.0954451	28.0000000	30.0000000
failure	6	3613.67	1052.37	2279.00	5289.00
guage	6	4222.50	716.8148296	3388.00	5289.00
E	6	1355388.33	123707.49	1172360.00	1502270.00

```
------------------------ length=4 width=0.75 vane=1.5 ------------------------
Variable      N            Mean         Std Dev         Minimum         Maximum
ffffffffffffffffffffffffffffffffffffffffffffffffffffffffffffffffffffffffffffff
density       8      39.9498504       3.0886800      34.8596533      43.7175639
angle         8      19.3750000       1.4078860      18.0000000      21.0000000
failure       8         3612.00     746.0279581         2603.00         4621.00
guage         8         5320.38         1070.60         3899.00         6966.00
E             8      1862676.25       555631.42      1240020.00      2886070.00
ffffffffffffffffffffffffffffffffffffffffffffffffffffffffffffffffffffffffffffff
-------------------------- length=4 width=1 vane=3 --------------------------
Variable      N            Mean         Std Dev         Minimum         Maximum
ffffffffffffffffffffffffffffffffffffffffffffffffffffffffffffffffffffffffffffff
density       9      39.4578836       1.0937850      37.1956607      40.6442698
angle         9      28.3333333       1.3228757      27.0000000      30.0000000
failure       9         3828.44     564.6275567         2558.00         4419.00
guage         9         4012.89     630.3955989         2558.00         4765.00
E             9      1353694.56       356405.95       968421.00      1915890.00
ffffffffffffffffffffffffffffffffffffffffffffffffffffffffffffffffffffffffffffff
------------------------- length=4 width=1 vane=1.5 -------------------------
Variable      N            Mean         Std Dev         Minimum         Maximum
ffffffffffffffffffffffffffffffffffffffffffffffffffffffffffffffffffffffffffffff
density       9      39.6597805       2.9666334      35.3544610      42.9597757
angle         9      17.6666667       0.5000000      17.0000000      18.0000000
failure       9         3876.56     655.9500955         3094.00         5374.00
guage         9         4967.00         1077.22         3094.00         6176.00
E             9      1803252.67       426627.70       979254.00      2382720.00
ffffffffffffffffffffffffffffffffffffffffffffffffffffffffffffffffffffffffffffff
```

This analysis is with the parallel tensile strength *based on a failure in the gauge length*.

This is more of a lower limit. The center portion of the specimen carried at least this much load.

Density and angle are the only significant sources of variation in this model.

```
Comparison of all Parallel Tension Data

                          The GLM Procedure
                      Class Level Information
                Class         Levels    Values
                length             3    4 8 12
                width              3    0.5 0.75 1
                vane               2    1.5 3
                   Number of observations    128
```

Dependent Variable: gauge

Source	DF	Sum of Squares	Mean Square	F Value	Pr > F
Model	6	74260492.6	12376748.8	38.67	**<.0001**
Error	121	38723621.6	320029.9		
Corrected Total	127	112984114.2			

R-Square	Coeff Var	Root MSE	gauge Mean
0.657265	10.89305	565.7119	5193.328

Source	DF	Type III SS	Mean Square	F Value	Pr > F
density	1	34851250.54	34851250.54	108.90	**<.0001**
angle	1	16455525.50	16455525.50	51.42	**<.0001**
length	2	1092049.96	546024.98	1.71	0.1859
width	2	326820.42	163410.21	0.51	0.6014

This analysis is the K-S test to see if strength at the actual failure location and assumed failure in the gauge length can be described by the same distribution. The null hypothesis is that the two sets of failure strengths can be described by the same distribution. This is accepted for p-values greater than 0.05. Otherwise, the distributions are statistically distinct. The p-value shows that these data sets are distinct.

Comparison of place of assumed failure

The NPAR1WAY Procedure

Kolmogorov-Smirnov Test for Variable strength

Classified by Variable type

type	N	EDF at Maximum	Deviation from Mean at Maximum
failure	128	0.687500	2.342291
gauge	128	0.273438	-2.342291
Total	256	0.480469	

Maximum Deviation Occurred at Observation 110

Value of strength at Maximum = 4621.0

Kolmogorov-Smirnov Two-Sample Test (Asymptotic)

KS 0.207031 D 0.414063

KSa 3.312500 **Pr > KSa <.0001**

Cramer-von Mises Test for Variable strength

Classified by Variable type

type	N	Summed Deviation from Mean
failure	128	2.101189
gauge	128	2.101189

Cramer-von Mises Statistics (Asymptotic)

CM 0.016416 CMa 4.202377

Kuiper Test for Variable strength

Classified by Variable type

type	N	Deviation from Mean
failure	128	0.414063
gauge	128	0.000000

Kuiper Two-Sample Test (Asymptotic)

K 0.414063 Ka 3.312500

Tension Transverse data

This analysis was run on the transverse tension data to find which factors were significant in a model E. Also included, following strength values, are the mean, standard deviation, min and max for each length, width and vane spacing combination. These statistics are provided for density, mean angle, E, strength at failure location (failure) and strength if failure occurred within gauge length (gauge). Length and angle are significant factors in the model, but density and width are not. The Tukey test was used to determine which lengths are significantly different. The 12-inch length is different from the 4-inch length.

Comparison of all Transverse Compression Data (outliers are removed)

The GLM Procedure

Class Level Information

Class	Levels	Values
length	3	4 8 12
width	3	0.5 0.75 1
vane	2	1.5 3

Number of observations 116

Dependent Variable: E

Source	DF	Sum of Squares	Mean Square	F Value	Pr > F
Model	6	168691001301	28115166884	13.54	**<.0001**
Error	109	226253732846	2075722319.7		
Corrected Total	115	394944734148			

R-Square	Coeff Var	Root MSE	E Mean
0.427126	47.22028	45560.10	96484.16

Source	DF	Type III SS	Mean Square	F Value	Pr > F
density	1	3475428271	3475428271	1.67	0.1984
angle	1	130936900405	130936900405	63.08	**<.0001**
length	2	34170555726	17085277863	8.23	**0.0005**
width	2	6440002429.8	3220001214.9	1.55	0.2166

Tukey's Studentized Range (HSD) Test for E

NOTE: This test controls the Type I experimentwise error rate.

Alpha	0.05
Error Degrees of Freedom	109
Error Mean Square	2.0757E9
Critical Value of Studentized Range	3.36043

Comparisons significant at the 0.05 level are indicated by ***.

length Comparison	Difference Between Means	Simultaneous 95% Confidence Limits		
4 - 8	17561	-5248	40370	
4 - 12	**40090**	**12620**	**67561**	***
8 - 4	-17561	-40370	5248	
8 - 12	22529	-3989	49047	
12 - 4	**-40090**	**-67561**	**-12620**	***
12 - 8	-22529	-49047	3989	

This analysis is for transverse tensile strength. The fist run is with strength calculated at the location of failure. This includes all of the grip failures that had stresses caused by more than pure tension. Tukey's test found that the 4 inch strands are different from the 8 and 12 inch strands. This analysis found length, angle and density all significant. Means based on panel type follow the GLM.

Comparison of all Transverse Tensile Strength Data

The GLM Procedure

Class Level Information

Class	Levels	Values
length	3	4 8 12
width	3	0.5 0.75 1
vane	2	1.5 3

Number of observations 116

Dependent Variable: failure

Source	DF	Sum of Squares	Mean Square	F Value	Pr > F
Model	6	3728784.921	621464.153	31.44	**<.0001**
Error	109	2154561.690	19766.621		
Corrected Total	115	5883346.611			

R-Square	Coeff Var	Root MSE	failure Mean
0.633786	28.60105	140.5938	491.5687

Source	DF	Type III SS	Mean Square	F Value	Pr > F
density	1	606537.039	606537.039	30.68	**<.0001**
angle	1	2223801.418	2223801.418	112.50	**<.0001**
length	2	135782.201	67891.101	3.43	**0.0358**
width	2	19611.543	9805.771	0.50	0.6103

Tukey's Studentized Range (HSD) Test for failure

NOTE: This test controls the Type I experimentwise error rate.

Alpha	0.05
Error Degrees of Freedom	109
Error Mean Square	19766.62
Critical Value of Studentized Range	3.36043

Comparisons significant at the 0.05 level are indicated by ***.

length Comparison	Difference Between Means	Simultaneous 95% Confidence Limits		
4 - 8	**154.39**	**84.00**	**224.77**	***
4 - 12	**176.99**	**92.22**	**261.76**	***
8 - 4	**-154.39**	**-224.77**	**-84.00**	***
8 - 12	22.61	-59.23	104.44	
12 - 4	**-176.99**	**-261.76**	**-92.22**	***
12 - 8	-22.61	-104.44	59.23	

---------- length=12 width=0.5 vane=3 ----------

Variable	N	Mean	Std Dev	Minimum	Maximum
density	8	39.1281846	1.9872767	36.6986441	42.0075217
angle	8	18.2500000	1.0350983	17.0000000	19.0000000
failure	8	413.7212500	172.3033116	177.4500000	639.2100000
gauge	8	425.8506250	155.9231017	205.4290000	639.2100000
E	8	92561.13	30562.26	43094.00	125436.00

---------- length=12 width=0.75 vane=3 ----------

Variable	N	Mean	Std Dev	Minimum	Maximum
density	9	39.6800555	1.3514831	37.8650714	41.8373601
angle	9	17.0000000	1.5000000	16.0000000	19.0000000
failure	9	482.6166667	60.0942574	349.1000000	565.4300000
gauge	9	489.2478889	60.2415832	349.1000000	565.4300000
E	9	64454.22	19785.91	37256.00	92778.00

---------- length=12 width=1 vane=3 ----------

Variable	N	Mean	Std Dev	Minimum	Maximum
density	8	39.4753618	4.7461344	31.5589331	44.5099093
angle	8	14.3750000	0.5175492	14.0000000	15.0000000
failure	8	353.5462500	96.0379034	247.3700000	539.1400000
gauge	8	366.0268750	91.2478260	252.9500000	539.1400000
E	8	61813.63	22477.97	38025.00	97349.00

---------- length=8 width=0.5 vane=3 ----------

Variable	N	Mean	Std Dev	Minimum	Maximum
density	9	39.4192901	2.7166743	35.8106523	44.6521047
angle	9	19.0000000	0.8660254	18.0000000	20.0000000
failure	9	592.9266667	133.4649215	311.4500000	752.6500000
gauge	9	624.0647778	152.8479992	311.4500000	772.2930000
E	9	141154.00	49977.23	63953.00	210351.00

---------- length=8 width=0.5 vane=1.5 ----------

Variable	N	Mean	Std Dev	Minimum	Maximum
density	8	38.7201714	1.9835426	35.8683954	41.7435378
angle	8	12.0000000	0	12.0000000	12.0000000
failure	8	309.8562500	88.5989939	163.8900000	427.1600000
gauge	8	326.1355000	75.2912722	209.2600000	427.1600000
E	8	53153.75	9288.37	38085.00	67918.00

```
------------------------- length=8 width=0.75 vane=3 -------------------------
Variable      N            Mean         Std Dev         Minimum         Maximum
ffffffffffffffffffffffffffffffffffffffffffffffffffffffffffffffffffffffffffffff
density       8      38.8790195       1.5217019      37.1760896      41.9344097
angle         8      17.5000000       0.9258201      17.0000000      19.0000000
failure       8     543.7837500     177.3359237     222.0100000     809.2500000
gauge         8     543.7837500     177.3359237     222.0100000     809.2500000
E             8       101935.63        74563.56        41454.00       279703.00
ffffffffffffffffffffffffffffffffffffffffffffffffffffffffffffffffffffffffffffff
------------------------- length=8 width=0.75 vane=1.5 -------------------------
Variable      N            Mean         Std Dev         Minimum         Maximum
ffffffffffffffffffffffffffffffffffffffffffffffffffffffffffffffffffffffffffffff
density       9      37.7364254       1.9961115      34.8832557      40.9294856
angle         9      12.6666667       1.3228757      11.0000000      14.0000000
failure       9     267.8255556      68.7509107     187.0300000     399.1300000
gauge         9     289.9327778      70.4051889     187.0300000     399.1300000
E             9        46060.67        18963.89        21534.00        74713.00
ffffffffffffffffffffffffffffffffffffffffffffffffffffffffffffffffffffffffffffff
--------------------------- length=8 width=1 vane=3 ----------------------------
Variable      N            Mean         Std Dev         Minimum         Maximum
ffffffffffffffffffffffffffffffffffffffffffffffffffffffffffffffffffffffffffffff
density       9      40.9841239       2.1276916      37.3076778      44.7562202
angle         9      18.3333333       0.5000000      18.0000000      19.0000000
failure       9     594.5155556     188.0253982     323.7500000     926.0600000
gauge         9     621.5097778     164.5632929     475.7490000     926.0600000
E             9       156679.44        95347.25        52847.00       314588.00
ffffffffffffffffffffffffffffffffffffffffffffffffffffffffffffffffffffffffffffff
------------------------- length=8 width=1 vane=1.5 --------------------------
Variable      N            Mean         Std Dev         Minimum         Maximum
ffffffffffffffffffffffffffffffffffffffffffffffffffffffffffffffffffffffffffffff
density       7      38.7053086       2.7238279      33.6000918      41.5536725
angle         7      13.5714286       0.5345225      13.0000000      14.0000000
failure       7     309.5900000     101.2957156     110.0700000     420.6400000
gauge         7     314.5681429      95.4325242     123.7720000     420.6400000
E             7        60123.43        22009.66        27187.00        84962.00
ffffffffffffffffffffffffffffffffffffffffffffffffffffffffffffffffffffffffffffff
------------------------- length=4 width=0.5 vane=3 --------------------------
Variable      N            Mean         Std Dev         Minimum         Maximum
ffffffffffffffffffffffffffffffffffffffffffffffffffffffffffffffffffffffffffffff
density       8      38.1030556       2.5387030      34.4575347      42.9503942
angle         8      28.3750000       1.6850180      27.0000000      31.0000000
failure       8     899.0787500     264.5283914     521.2500000         1324.44
gauge         8     929.2225000     274.8440400     521.2500000         1324.44
E             8       161283.38        45583.61        92062.00       223763.00
ffffffffffffffffffffffffffffffffffffffffffffffffffffffffffffffffffffffffffffff
------------------------- length=4 width=0.5 vane=1.5 ------------------------
Variable      N            Mean         Std Dev         Minimum         Maximum
ffffffffffffffffffffffffffffffffffffffffffffffffffffffffffffffffffffffffffffff
density       8      38.2620278       1.4991205      36.8839005      40.7639680
angle         8      18.1250000       0.8345230      17.0000000      19.0000000
failure       8     435.7262500      98.5219187     299.0000000     631.6200000
gauge         8     456.0057500      88.3438581     364.8200000     652.5770000
E             8        76592.75        16573.58        54892.00       100223.00
ffffffffffffffffffffffffffffffffffffffffffffffffffffffffffffffffffffffffffffff
```

```
-------------------------- length=4 width=0.75 vane=3 --------------------------
Variable      N            Mean         Std Dev         Minimum         Maximum
ffffffffffffffffffffffffffffffffffffffffffffffffffffffffffffffffffffffffffffffff
density       6      37.6228841       0.4253912      36.9550861      38.0854136
angle         6      28.3333333       0.8164966      28.0000000      30.0000000
failure       6     735.0633333     195.1752067     453.4300000     964.8600000
gauge         6     792.7580000     182.6070983     453.4300000     964.8600000
E             6       165655.50        66962.24        81613.00       266154.00
ffffffffffffffffffffffffffffffffffffffffffffffffffffffffffffffffffffffffffffffff
------------------------- length=4 width=0.75 vane=1.5 -------------------------
Variable      N            Mean         Std Dev         Minimum         Maximum
ffffffffffffffffffffffffffffffffffffffffffffffffffffffffffffffffffffffffffffffff
density       6      38.1208837       1.4794308      36.2762907      39.9068588
angle         6      19.8333333       1.3291601      18.0000000      21.0000000
failure       6     418.2750000     162.3352940     227.7900000     592.9500000
gauge         6     457.3741667     174.1260625     268.2110000     631.6180000
E             6        71918.50        26954.96        44002.00       119414.00
ffffffffffffffffffffffffffffffffffffffffffffffffffffffffffffffffffffffffffffffff
--------------------------- length=4 width=1 vane=3 ----------------------------
Variable      N            Mean         Std Dev         Minimum         Maximum
ffffffffffffffffffffffffffffffffffffffffffffffffffffffffffffffffffffffffffffffff
density       5      37.4196378       2.5430811      34.2719774      39.7442219
angle         5      28.0000000       1.2247449      27.0000000      30.0000000
failure       5     773.1000000     240.3962297     345.0700000     917.6600000
gauge         5     773.1000000     240.3962297     345.0700000     917.6600000
E             5       137172.60        19132.73       104415.00       150947.00
ffffffffffffffffffffffffffffffffffffffffffffffffffffffffffffffffffffffffffffffff
-------------------------- length=4 width=1 vane=1.5 ---------------------------
Variable      N            Mean         Std Dev         Minimum         Maximum
ffffffffffffffffffffffffffffffffffffffffffffffffffffffffffffffffffffffffffffffff
density       8      38.5634310       1.3829428      35.9528382      40.4770056
angle         8      17.6250000       0.5175492      17.0000000      18.0000000
failure       8     372.8312500      94.7305438     190.0000000     497.0000000
gauge         8     406.0068750      73.8046162     278.2340000     497.0000000
E             8        75766.88        16910.81        48813.00        99927.00
ffffffffffffffffffffffffffffffffffffffffffffffffffffffffffffffffffffffffffffffff
```

This analysis is with the strength based on a failure in the gauge length. This is more of a lower limit. The center portion of the specimen carried at least this much load. Density, length and angle are significant sources of variation in this model. 4” is different from 8” and 12”.

```
Comparison of all Transverse Tensile Strength Data

                               The GLM Procedure
                            Class Level Information
                      Class         Levels    Values
                      length             3    4 8 12
                      width              3    0.5 0.75 1
                      vane               2    1.5 3
                         Number of observations    116
```

Dependent Variable: gauge

Source	DF	Sum of Squares	Mean Square	F Value	Pr > F
Model	6	3898438.303	649739.717	33.99	**<.0001**
Error	109	2083605.910	19115.651		
Corrected Total	115	5982044.214			

R-Square	Coeff Var	Root MSE	gauge Mean
0.651690	26.99318	138.2594	512.2011

Source	DF	Type III SS	Mean Square	F Value	Pr > F
density	1	626854.797	626854.797	32.79	**<.0001**
angle	1	2220084.555	2220084.555	116.14	**<.0001**
length	2	128256.358	64128.179	3.35	**0.0386**
width	2	24348.851	12174.425	0.64	0.5309

Tukey's Studentized Range (HSD) Test for gauge
NOTE: This test controls the Type I experimentwise error rate.

Alpha	0.05
Error Degrees of Freedom	109
Error Mean Square	19115.65
Critical Value of Studentized Range	3.36043

Comparisons significant at the 0.05 level are indicated by ***.

length Comparison	Difference Between Means	Simultaneous 95% Confidence Limits		
4 - 8	**167.12**	**97.90**	**236.34**	***
4 - 12	**197.21**	**113.84**	**280.57**	***
8 - 4	**-167.12**	**-236.34**	**-97.90**	***
8 - 12	30.09	-50.38	110.56	
12 - 4	**-197.21**	**-280.57**	**-113.84**	***
12 - 8	-30.09	-110.56	50.38	

This analysis is the K-S test to see if failure and gauge can be described by the same distribution. The null hypothesis is that the two sets of failure strengths can be described by the same distribution. This is accepted for p-values greater than 0.05. Otherwise, the distributions are statistically distinct. The p-value shows that these data sets are not distinct. This may be a result of few grip-line failures (less difference between assumed and real failures).

Comparison of Failure Data

The NPAR1WAY Procedure

Kolmogorov-Smirnov Test for Variable strength

Classified by Variable type

type	N	EDF at Maximum	Deviation from Mean at Maximum
failure	116	0.155172	0.371391
gauge	116	0.086207	-0.371391
Total	232	0.120690	

Maximum Deviation Occurred at Observation 99

Value of strength at Maximum = 269.070

Kolmogorov-Smirnov Two-Sample Test (Asymptotic)

KS	0.034483	D	0.068966
KSa	0.525226	**Pr > KSa**	**0.9455**

Cramer-von Mises Test for Variable strength

Classified by Variable type

type	N	Summed Deviation from Mean
failure	116	0.024599
gauge	116	0.024599

Cramer-von Mises Statistics (Asymptotic)

CM	0.000212	CMa	0.049197

Kuiper Test for Variable strength

Classified by Variable type

type	N	Deviation from Mean
failure	116	0.068966
gauge	116	0.000000

Kuiper Two-Sample Test (Asymptotic)

K	0.068966	Ka	0.525226	Pr	

APPENDIX H: MATHEMATICA PROGRAMS

The following Mathematica programs were utilized for various modeling tasks. The first program was used to determine Young's modulus, E from stress strain curves. The second, third and fourth programs were used to transform parallel properties using tensor transformation and mean angle, the normal distribution and the 2-parameter Weibull distribution, respectively. The fifth, sixth and seventh are the same angular descriptors, but transformation was completed using Hankinson's equation.

Program 1:

```
<< Statistics`NonlinearFit`
model = g + a x + b x^2 + c x^3 + d x^4;
data = Import["D:\data\compression_par\sample_15´5", "Table"];
n = Length[data]
temp2 = Take[data, {2, n, 1}];
temp = Array[aa, {Length[temp2], 2}];
temp[[All, 2]] = temp2[[All, 2]];
temp[[All, 1]] = temp2[[All, 1]];
ListPlot[temp];
For[i = 1, temp[[i, 1]] < 0.015, i++]
i
w1 = 2.044;
w2 = 2.048;
t = 0.807;
guage = (3.031 + 3.049 + 3.011 + 3.030) / 4;
w = (w1 + w2) / 2;
mx = Max[temp[[All, 2]]];
mxstress = mx / (w t)
```

```
data2 = Take[data, {2, i, 1}];
data3 = Array[a, {Length[data2], 2}];
data3[[All, 2]] = data2[[All, 2]] / (w * t);
data3[[All, 1]] = data2[[All, 1]] / guage;
stressstraincurve = ListPlot[data3, PlotJoined -> True, PlotStyle → Hue[.6]];
fiteq = NonlinearFit[data3, model, x, {g, a, b, c, d}]
linfit = Fit[data3, {1, x}, x]
d1 = ∂x fiteq
d2 = ∂x d1
Solve[Dt[d1, x] == 0, x]
Solve[Dt[d2, x] == 0, x]
plotfit = Plot[{fiteq}, {x, 0, 0.005}];
Show[stressstraincurve, plotfit];

d1 /. x → 0.0034
Plot[d1, {x, 0, .010}];
d2 = Chop[Dt[d1, x]]
Plot[d2, {x, 0, .010}];
```

Program 2:

```
E1 = 1721000;
E2 = 86090;
G12 = 95180;
nu = 0.49;
angle = (18.31) * Pi / 180;
S11 = N[1 / E1];
S22 = N[1 / E2];
S12 = N[-nu / E1];
S66 = N[1 / G12];
Sbar11 = S11 * (Cos[angle]) ^4 +
    (2 * S12 + S66) * (Sin[angle]) ^2 *
     (Cos[angle]) ^2 + S22 * (Sin[angle]) ^4;
Ex = 1 / Sbar11
Sbar22 = S11 * (Sin[angle]) ^4 +
    (2 * S12 + S66) * (Sin[angle]) ^2 *
     (Cos[angle]) ^2 + S22 (Cos[angle]) ^4;
Ey = 1 / Sbar22
```

Program 3:

```
mean = 89.4334;
stdev = 19.1165;
Ex = 19374;
Ey = 969;
Gxy = 1071;
nu = 0.49;
S11 = N[1 / Ex];
S22 = N[1 / Ey];
S12 = N[-nu / Ex];
S66 = N[1 / Gxy];
prob5 =
  N[2 * Integrate[1 / (stdev * (2 * Pi) ^0.5) * Exp[-0.5 ((x - mean) / stdev) ^2], {x, 0, 10}]];
prob15 =
  N[2 * Integrate[1 / (stdev * (2 * Pi) ^0.5) * Exp[-0.5 ((x - mean) / stdev) ^2], {x, 10, 20}]];
prob25 =
  N[2 * Integrate[1 / (stdev * (2 * Pi) ^0.5) * Exp[-0.5 ((x - mean) / stdev) ^2], {x, 20, 30}]];
prob35 =
  N[2 * Integrate[1 / (stdev * (2 * Pi) ^0.5) * Exp[-0.5 ((x - mean) / stdev) ^2], {x, 30, 40}]];
prob45 =
  N[2 * Integrate[1 / (stdev * (2 * Pi) ^0.5) * Exp[-0.5 ((x - mean) / stdev) ^2], {x, 40, 50}]];
prob55 =
  N[2 * Integrate[1 / (stdev * (2 * Pi) ^0.5) * Exp[-0.5 ((x - mean) / stdev) ^2], {x, 50, 60}]];
prob65 =
  N[2 * Integrate[1 / (stdev * (2 * Pi) ^0.5) * Exp[-0.5 ((x - mean) / stdev) ^2], {x, 60, 70}]];
prob75 =
  N[2 * Integrate[1 / (stdev * (2 * Pi) ^0.5) * Exp[-0.5 ((x - mean) / stdev) ^2], {x, 70, 80}]];
prob85 =
 N[2 * Integrate[1 / (stdev * (2 * Pi) ^0.5) * Exp[-0.5 ((x - mean) / stdev) ^2], {x, 80, 90}]
```

```
S5bar11 =
  N[S11*(Cos[5*Pi/180])^4 +
    (2*S12 + S66) *(Sin[5*Pi/180])^2*(Cos[5*Pi/180])^2 +
    S22*(Sin[5*Pi/180])^4];
E5 = N[1/S5bar11* prob85];
S15bar11 =
  N[S11*(Cos[15*Pi/180])^4 +
    (2*S12 + S66) *(Sin[15*Pi/180])^2*(Cos[15*Pi/180])^2 +
    S22*(Sin[15*Pi/180])^4];
E15 = N[1/S15bar11* prob75];
S25bar11 =
  N[S11*(Cos[25*Pi/180])^4 +
    (2*S12 + S66) *(Sin[25*Pi/180])^2*(Cos[25*Pi/180])^2 +
    S22*(Sin[25*Pi/180])^4];
E25 = N[1/S25bar11* prob65];
S35bar11 =
  N[S11*(Cos[35*Pi/180])^4 +
    (2*S12 + S66) *(Sin[35*Pi/180])^2*(Cos[35*Pi/180])^2 +
    S22*(Sin[35*Pi/180])^4];
E35 = N[1/S35bar11* prob55];
S45bar11 =
  N[S11*(Cos[45*Pi/180])^4 +
    (2*S12 + S66) *(Sin[45*Pi/180])^2*(Cos[45*Pi/180])^2 +
    S22*(Sin[45*Pi/180])^4];
E45 = N[1/S45bar11* prob45];
S55bar11 =
  N[S11*(Cos[55*Pi/180])^4 +
    (2*S12 + S66) *(Sin[55*Pi/180])^2*(Cos[55*Pi/180])^2 +
    S22*(Sin[55*Pi/180])^4];
```

```
E55 = N[1 / S55bar11 * prob35];
S65bar11 =
  N[S11 * (Cos[65 * Pi / 180]) ^4 +
    (2 * S12 + S66) * (Sin[65 * Pi / 180]) ^2 * (Cos[65 * Pi / 180]) ^2 +
    S22 * (Sin[65 * Pi / 180]) ^4];
E65 = N[1 / S65bar11 * prob25];
S75bar11 =
  N[S11 * (Cos[75 * Pi / 180]) ^4 +
    (2 * S12 + S66) * (Sin[75 * Pi / 180]) ^2 * (Cos[75 * Pi / 180]) ^2 +
    S22 * (Sin[75 * Pi / 180]) ^4];
E75 = N[1 / S75bar11 * prob15];
S85bar11 =
  N[S11 * (Cos[85 * Pi / 180]) ^4 +
    (2 * S12 + S66) * (Sin[85 * Pi / 180]) ^2 * (Cos[85 * Pi / 180]) ^2 +
    S22 * (Sin[85 * Pi / 180]) ^4];
E85 = N[1 / S85bar11 * prob5];
Extrans = N[E5 + E15 + E25 + E35 + E45 + E55 + E65 + E75 + E85]

S5bar22 = S11 * (Sin[5 * Pi / 180]) ^4 +
   (2 * S12 + S66) * (Sin[5 * Pi / 180]) ^2 * (Cos[5 * Pi / 180]) ^2 +
   S22 (Cos[5 * Pi / 180]) ^4;
Ey5 = N[1 / S5bar22 * prob85];
S15bar22 = S11 * (Sin[15 * Pi / 180]) ^4 +
   (2 * S12 + S66) * (Sin[15 * Pi / 180]) ^2 * (Cos[15 * Pi / 180]) ^2 +
   S22 (Cos[15 * Pi / 180]) ^4;
Ey15 = N[1 / S15bar22 * prob75];
```

```
S25bar22 = S11 * (Sin[25 * Pi / 180]) ^4 +
    (2 * S12 + S66) * (Sin[25 * Pi / 180]) ^2 * (Cos[25 * Pi / 180]) ^2 +
    S22 (Cos[25 * Pi / 180]) ^4;
Ey25 = N[1 / S25bar22 * prob65];
S35bar22 = S11 * (Sin[35 * Pi / 180]) ^4 +
    (2 * S12 + S66) * (Sin[35 * Pi / 180]) ^2 * (Cos[35 * Pi / 180]) ^2 +
    S22 (Cos[35 * Pi / 180]) ^4;
Ey35 = N[1 / S35bar22 * prob55];
S45bar22 = S11 * (Sin[45 * Pi / 180]) ^4 +
    (2 * S12 + S66) * (Sin[45 * Pi / 180]) ^2 * (Cos[45 * Pi / 180]) ^2 +
    S22 (Cos[45 * Pi / 180]) ^4;
Ey45 = N[1 / S45bar22 * prob45];
S55bar22 = S11 * (Sin[55 * Pi / 180]) ^4 +
    (2 * S12 + S66) * (Sin[55 * Pi / 180]) ^2 * (Cos[55 * Pi / 180]) ^2 +
    S22 (Cos[55 * Pi / 180]) ^4;
Ey55 = N[1 / S55bar22 * prob35];
S65bar22 = S11 * (Sin[65 * Pi / 180]) ^4 +
    (2 * S12 + S66) * (Sin[65 * Pi / 180]) ^2 * (Cos[65 * Pi / 180]) ^2 +
    S22 (Cos[65 * Pi / 180]) ^4;
Ey65 = N[1 / S65bar22 * prob25];
S75bar22 = S11 * (Sin[75 * Pi / 180]) ^4 +
    (2 * S12 + S66) * (Sin[75 * Pi / 180]) ^2 * (Cos[75 * Pi / 180]) ^2 +
    S22 (Cos[75 * Pi / 180]) ^4;
Ey75 = N[1 / S75bar22 * prob15];
S85bar22 = S11 * (Sin[85 * Pi / 180]) ^4 +
    (2 * S12 + S66) * (Sin[85 * Pi / 180]) ^2 * (Cos[85 * Pi / 180]) ^2 +
    S22 (Cos[85 * Pi / 180]) ^4;
Ey85 = N[1 / S85bar22 * prob5];
Eytrans = Ey5 + Ey15 + Ey25 + Ey35 + Ey45 + Ey55 + Ey65 + Ey75 + Ey85
E5
1 / S5bar22
```

Program 4:

```
scale = 98.7194;
shape = 4.0975;
Ex = 2810000;
Ey = 140600;
Gxy = 155400;
nu = 0.49;
S11 = N[1/Ex];
S22 = N[1/Ey];
S12 = N[-nu/Ex];
S66 = N[1/Gxy];
prob5 = N[1-Exp[-(5/scale)^shape]];
tprob15 = N[1-Exp[-(15/scale)^shape]];
prob15 = tprob15-prob5;
tprob25 = N[1-Exp[-(25/scale)^shape]];
prob25 = tprob25-tprob15;
tprob35 = N[1-Exp[-(35/scale)^shape]];
prob35 = tprob35-tprob25;
tprob45 = N[1-Exp[-(45/scale)^shape]];
prob45 = tprob45-tprob35;
tprob55 = N[1-Exp[-(55/scale)^shape]];
prob55 = tprob55-tprob45;
tprob65 = N[1-Exp[-(65/scale)^shape]];
prob65 = tprob65-tprob55;
tprob75 = N[1-Exp[-(75/scale)^shape]];
prob75 = tprob75-tprob65;
tprob85 = N[1-Exp[-(85/scale)^shape]];
prob85 = tprob85-tprob75;
tprob95 = N[1-Exp[-(95/scale)^shape]];
prob95 = tprob95-tprob85;
tprob105 = N[1-Exp[-(105/scale)^shape]];
prob105 = tprob105-tprob95;
tprob115 = N[1-Exp[-(115/scale)^shape]];
prob115 = tprob115-tprob105;
tprob125 = N[1-Exp[-(125/scale)^shape]];
prob125 = tprob125-tprob115;
tprob135 = N[1-Exp[-(135/scale)^shape]];
prob135 = tprob135-tprob125;
tprob145 = N[1-Exp[-(145/scale)^shape]];
prob145 = tprob145-tprob135;
```

```
tprob155 = N[1 - Exp[-(155 / scale)^shape]];
prob155 = tprob155 - tprob145;
tprob165 = N[1 - Exp[-(165 / scale)^shape]];
prob165 = tprob165 - tprob155;
tprob175 = N[1 - Exp[-(175 / scale)^shape]];
prob175 = tprob175 - tprob165;
tprobtotal = prob5 + prob15 + prob25 + prob35 + prob45 + prob55 + prob65 +
   prob75 + prob85 + prob95 + prob105 + prob115 + prob125 + prob135 + prob145 +
   prob155 + prob165 + prob175;
S5bar11 =
  N[S11 * (Cos[5 * Pi / 180])^4 + (2 * S12 + S66) * (Sin[5 * Pi / 180])^2 *
     (Cos[5 * Pi / 180])^2 + S22 * (Sin[5 * Pi / 180])^4];
E5 = N[1 / S5bar11 * prob85];
S15bar11 =
  N[S11 * (Cos[15 * Pi / 180])^4 + (2 * S12 + S66) * (Sin[15 * Pi / 180])^2 *
     (Cos[15 * Pi / 180])^2 + S22 * (Sin[15 * Pi / 180])^4];
E15 = N[1 / S15bar11 * prob75];
S25bar11 =
  N[S11 * (Cos[25 * Pi / 180])^4 + (2 * S12 + S66) * (Sin[25 * Pi / 180])^2 *
     (Cos[25 * Pi / 180])^2 + S22 * (Sin[25 * Pi / 180])^4];
E25 = N[1 / S25bar11 * prob65];
S35bar11 =
  N[S11 * (Cos[35 * Pi / 180])^4 + (2 * S12 + S66) * (Sin[35 * Pi / 180])^2 *
     (Cos[35 * Pi / 180])^2 + S22 * (Sin[35 * Pi / 180])^4];
E35 = N[1 / S35bar11 * prob55];
S45bar11 =
  N[S11 * (Cos[45 * Pi / 180])^4 + (2 * S12 + S66) * (Sin[45 * Pi / 180])^2 *
     (Cos[45 * Pi / 180])^2 + S22 * (Sin[45 * Pi / 180])^4];
E45 = N[1 / S45bar11 * prob45];
S55bar11 =
  N[S11 * (Cos[55 * Pi / 180])^4 + (2 * S12 + S66) * (Sin[55 * Pi / 180])^2 *
     (Cos[55 * Pi / 180])^2 + S22 * (Sin[55 * Pi / 180])^4];
```

```
S65bar11 =
  N[S11 * (Cos[65 * Pi / 180]) ^4 + (2 * S12 + S66) * (Sin[65 * Pi / 180]) ^2 *
     (Cos[65 * Pi / 180]) ^2 + S22 * (Sin[65 * Pi / 180]) ^4];
E65 = N[1 / S5bar11 * prob25];
S75bar11 =
  N[S11 * (Cos[75 * Pi / 180]) ^4 + (2 * S12 + S66) * (Sin[75 * Pi / 180]) ^2 *
     (Cos[75 * Pi / 180]) ^2 + S22 * (Sin[75 * Pi / 180]) ^4];
E75 = N[1 / S75bar11 * prob15];
S85bar11 =
  N[S11 * (Cos[85 * Pi / 180]) ^4 + (2 * S12 + S66) * (Sin[85 * Pi / 180]) ^2 *
     (Cos[85 * Pi / 180]) ^2 + S22 * (Sin[85 * Pi / 180]) ^4];
E85 = N[1 / S85bar11 * prob5];
E95 = N[1 / S85bar11 * prob175];
E105 = N[1 / S75bar11 * prob165];
E115 = N[1 / S65bar11 * prob155];
E125 = N[1 / S55bar11 * prob145];
E135 = N[1 / S45bar11 * prob135];
E145 = N[1 / S35bar11 * prob125];
E155 = N[1 / S25bar11 * prob115];
E165 = N[1 / S15bar11 * prob105];
E175 = N[1 / S5bar11 * prob95];
Extrans = E5 + E15 + E25 + E35 + E45 + E55 + E65 + E75 + E85 + E95 + E105 + E115 +
  E125 + E135 + E145 + E155 + E165 + E175
S5bar22 = S11 * (Sin[5 * Pi / 180]) ^4 +
   (2 * S12 + S66) * (Sin[5 * Pi / 180]) ^2 * (Cos[5 * Pi / 180]) ^2 + S22 (Cos[5 * Pi / 180]) ^4;
Ey5 = N[1 / S5bar22 * prob85];
S15bar22 = S11 * (Sin[15 * Pi / 180]) ^4 +
   (2 * S12 + S66) * (Sin[15 * Pi / 180]) ^2 * (Cos[15 * Pi / 180]) ^2 +
   S22 (Cos[15 * Pi / 180]) ^4;
Ey15 = N[1 / S15bar22 * prob75];
S25bar22 = S11 * (Sin[25 * Pi / 180]) ^4 +
   (2 * S12 + S66) * (Sin[25 * Pi / 180]) ^2 * (Cos[25 * Pi / 180]) ^2 +
   S22 (Cos[25 * Pi / 180]) ^4;
Ey25 = N[1 / S25bar22 * prob65];
S35bar22 = S11 * (Sin[35 * Pi / 180]) ^4 +
   (2 * S12 + S66) * (Sin[35 * Pi / 180]) ^2 * (Cos[35 * Pi / 180]) ^2 +
   S22 (Cos[35 * Pi / 180]) ^4;
Ey35 = N[1 / S35bar22 * prob55];
S45bar22 = S11 * (Sin[45 * Pi / 180]) ^4 +
   (2 * S12 + S66) * (Sin[45 * Pi / 180]) ^2 * (Cos[45 * Pi / 180]) ^2 +
   S22 (Cos[45 * Pi / 180]) ^4;
```

```
S55bar22 = S11*(Sin[55*Pi/180])^4 +
    (2*S12 + S66) *(Sin[55*Pi/180])^2*(Cos[55*Pi/180])^2 +
    S22 (Cos[55*Pi/180])^4;
Ey55 = N[1/S55bar22*prob35];
S65bar22 = S11*(Sin[65*Pi/180])^4 +
    (2*S12 + S66) *(Sin[65*Pi/180])^2*(Cos[65*Pi/180])^2 +
    S22 (Cos[65*Pi/180])^4;
Ey65 = N[1/S65bar22*prob25];
S75bar22 = S11*(Sin[75*Pi/180])^4 +
    (2*S12 + S66) *(Sin[75*Pi/180])^2*(Cos[75*Pi/180])^2 +
    S22 (Cos[75*Pi/180])^4;
Ey75 = N[1/S75bar22*prob15];
S85bar22 = S11*(Sin[85*Pi/180])^4 +
    (2*S12 + S66) *(Sin[85*Pi/180])^2*(Cos[85*Pi/180])^2 +
    S22 (Cos[85*Pi/180])^4;
Ey85 = N[1/S85bar22*prob5];
Ey85 = N[1/S85bar22*prob5];
Ey95 = N[1/S85bar22*prob175];
Ey105 = N[1/S75bar22*prob165];
Ey115 = N[1/S65bar22*prob155];
Ey125 = N[1/S55bar22*prob145];
Ey135 = N[1/S45bar22*prob135];
Ey145 = N[1/S35bar22*prob125];
Ey155 = N[1/S25bar22*prob115];
Ey165 = N[1/S15bar22*prob105];
Ey175 = N[1/S5bar22*prob95];
Eytrans = Ey5 + Ey15 + Ey25 + Ey35 + Ey45 + Ey55 + Ey65 + Ey75 + Ey85 + Ey95 +
  Ey105 + Ey115 + Ey125 + Ey135 + Ey145 + Ey155 + Ey165 + Ey175
```

Program 5:

```
E1 = 2810000;
E2 = 140600;
G12 = 155400;
nu = 0.49;
n = 2;
meanangle = (18.39)*Pi/180;
Etrans =
 N[
  (E1*E2) /
   (E1*(Sin[meanangle])^n + E2*(Cos[meanangle])^n)]
```

```
density = 40;
SG = density / 62.4;
E1 = 2.39 * SG^0.7 * 10^6
E2 = 200000;
G12 = 100000;
nu = 0.3;
n = 2;
meanangle = (20) * Pi / 180;
Etrans =
 N[(E1 * E2) / (E1 * Sin[meanangle]^n + E2 * Cos[meanangle]^n)]
```

Program 6:

```
mean = 90.0218;
stdev = 23.6939;
E1 = 1721000;
E2 = 86090;
n = 2;
prob5 =
  N[
   2 * ∫_0^10 1 / (stdev * (2 * Pi) ^0.5) *
       Exp[-0.5 ((x - mean) / stdev) ^2] dx];
hank85 =
  N[
   (E1 * E2) /
    (E1 * Sin[85 * Pi / 180] ^n + E2 * Cos[85 * Pi / 180] ^n)];
E5 = prob5 * hank85;
prob15 =
  N[
   2 * ∫_10^20 1 / (stdev * (2 * Pi) ^0.5) *
       Exp[-0.5 ((x - mean) / stdev) ^2] dx];
hank75 =
  N[
   (E1 * E2) /
    (E1 * Sin[75 * Pi / 180] ^n + E2 * Cos[75 * Pi / 180] ^n)];
E15 = prob15 * hank75;
prob25 =
  N[
   2 * ∫_20^30 1 / (stdev * (2 * Pi) ^0.5) *
       Exp[-0.5 ((x - mean) / stdev) ^2] dx];
hank65 =
  N[
   (E1 * E2) /
    (E1 * Sin[65 * Pi / 180] ^n + E2 * Cos[65 * Pi / 180] ^n)];
E25 = prob25 * hank65;
```

```
prob35 =
  N[
   2* ∫_30^40 1/(stdev*(2*Pi)^0.5) *
      Exp[-0.5((x - mean)/stdev)^2] dx];
hank55 =
  N[
   (E1*E2)/
    (E1*Sin[55*Pi/180]^n + E2*Cos[55*Pi/180]^n)];
E35 = prob35*hank55;
prob45 =
  N[
   2* ∫_40^50 1/(stdev*(2*Pi)^0.5) *
      Exp[-0.5((x - mean)/stdev)^2] dx];
hank45 =
  N[
   (E1*E2)/
    (E1*Sin[45*Pi/180]^n + E2*Cos[45*Pi/180]^n)];
E45 = prob45*hank45;
prob55 =
  N[
   2* ∫_50^60 1/(stdev*(2*Pi)^0.5) *
      Exp[-0.5((x - mean)/stdev)^2] dx];
hank35 =
  N[
   (E1*E2)/
    (E1*Sin[35*Pi/180]^n + E2*Cos[35*Pi/180]^n)];
E55 = prob55*hank35;
prob65 =
  N[
   2* ∫_60^70 1/(stdev*(2*Pi)^0.5) *
      Exp[-0.5((x - mean)/stdev)^2] dx];
hank25 =
  N[
   (E1*E2)/
    (E1*Sin[25*Pi/180]^n + E2*Cos[25*Pi/180]^n)];
E65 = prob65*hank25;
```

```
prob75 =
  N[
   2* ∫_70^80 1/(stdev*(2*Pi)^0.5) *
      Exp[-0.5((x - mean)/stdev)^2] dx];
hank15 =
  N[
   (E1*E2)/
    (E1*Sin[15*Pi/180]^n + E2*Cos[15*Pi/180]^n)];
E75 = prob75*hank15;
prob85 =
  N[
   2* ∫_80^90 1/(stdev*(2*Pi)^0.5) *
      Exp[-0.5((x - mean)/stdev)^2] dx];
hank5 =
  N[
   (E1*E2)/
    (E1*Sin[5*Pi/180]^n + E2*Cos[5*Pi/180]^n)];
E85 = prob85*hank5;
Etrans = E5 + E15 + E25 + E35 + E45 + E55 + E65 + E75 + E85
```

Program 7:

```
scale = 100.8918;
shape = 2.7377;
E1 = 2810000;
E2 = 140600;
n = 2;
prob5 = N[1 - Exp[-(5 / scale)^shape]];
tprob15 = N[1 - Exp[-(15 / scale)^shape]];
prob15 = tprob15 - prob5;
tprob25 = N[1 - Exp[-(25 / scale)^shape]];
prob25 = tprob25 - tprob15;
tprob35 = N[1 - Exp[-(35 / scale)^shape]];
prob35 = tprob35 - tprob25;
tprob45 = N[1 - Exp[-(45 / scale)^shape]];
prob45 = tprob45 - tprob35;
tprob55 = N[1 - Exp[-(55 / scale)^shape]];
prob55 = tprob55 - tprob45;
tprob65 = N[1 - Exp[-(65 / scale)^shape]];
prob65 = tprob65 - tprob55;
tprob75 = N[1 - Exp[-(75 / scale)^shape]];
prob75 = tprob75 - tprob65;
tprob85 = N[1 - Exp[-(85 / scale)^shape]];
prob85 = tprob85 - tprob75;
tprob95 = N[1 - Exp[-(95 / scale)^shape]];
prob95 = tprob95 - tprob85;
tprob105 = N[1 - Exp[-(105 / scale)^shape]];
prob105 = tprob105 - tprob95;
```

```
tprob115 = N[1 - Exp[-(115 / scale)^shape]];
prob115 = tprob115 - tprob105;
tprob125 = N[1 - Exp[-(125 / scale)^shape]];
prob125 = tprob125 - tprob115;
tprob135 = N[1 - Exp[-(135 / scale)^shape]];
prob135 = tprob135 - tprob125;
tprob145 = N[1 - Exp[-(145 / scale)^shape]];
prob145 = tprob145 - tprob135;
tprob155 = N[1 - Exp[-(155 / scale)^shape]];
prob155 = tprob155 - tprob145;
tprob165 = N[1 - Exp[-(165 / scale)^shape]];
prob165 = tprob165 - tprob155;
tprob175 = N[1 - Exp[-(175 / scale)^shape]];
prob175 = tprob175 - tprob165;
tprobtotal = prob5 + prob15 + prob25 + prob35 + prob45 +
    prob55 + prob65 + prob75 + prob85 + prob95 + prob105 +
    prob115 + prob125 + prob135 + prob145 + prob155 +
    prob165 + prob175;
hank5 =
  N[
   (E1 * E2) /
    (E1 * Sin[5 * Pi / 180]^n + E2 * Cos[5 * Pi / 180]^n)];
hank15 =
  N[
   (E1 * E2) /
    (E1 * Sin[15 * Pi / 180]^n + E2 * Cos[15 * Pi / 180]^n)];
```

```
hank25 =
  N[
   (E1 * E2) /
    (E1 * Sin[25 * Pi / 180] ^n + E2 * Cos[25 * Pi / 180] ^n)];
hank35 =
  N[
   (E1 * E2) /
    (E1 * Sin[35 * Pi / 180] ^n + E2 * Cos[35 * Pi / 180] ^n)];
hank45 =
  N[
   (E1 * E2) /
    (E1 * Sin[45 * Pi / 180] ^n + E2 * Cos[45 * Pi / 180] ^n)];
hank55 =
  N[
   (E1 * E2) /
    (E1 * Sin[55 * Pi / 180] ^n + E2 * Cos[55 * Pi / 180] ^n)];
hank65 =
  N[
   (E1 * E2) /
    (E1 * Sin[65 * Pi / 180] ^n + E2 * Cos[65 * Pi / 180] ^n)];
hank75 =
  N[
   (E1 * E2) /
    (E1 * Sin[75 * Pi / 180] ^n + E2 * Cos[75 * Pi / 180] ^n)];
hank85 =
  N[
   (E1 * E2) /
    (E1 * Sin[85 * Pi / 180] ^n + E2 * Cos[85 * Pi / 180] ^n)];
Etrans = prob5 * hank85 + prob15 * hank75 + prob25 * hank65 +
  prob35 * hank55 + prob45 * hank45 + prob55 * hank35 +
  prob65 * hank25 + prob75 * hank15 + prob85 * hank5 +
  prob95 * hank5 + prob105 * hank15 + prob115 * hank25 +
  prob125 * hank35 + prob135 * hank45 + prob145 * hank55 +
  prob155 * hank65 + prob165 * hank75 + prob175 * hank85
```

APPENDIX I: SAS PROGRAMS

The following programs were used in SAS to perform the statistical analysis. The first program is a general linear model that assumes no significant interactions and identifies significant factors influencing the model. It also uses the Tukey test to identify differences in lengths. The second program compares samples of data to see if they are described by the same distribution using the Kolmgorov-Smirnov 2-sample test. Finally, the last program fits the normal and 2-parameter Weibull distributions to a set of data. This program returns the descriptive parameters, goodness of fit statistics and histograms.

Program 1:

```
options linesize=80 pageno=1;
 data full;
 input density angle E length width vane strength;
 cards;
title 'Comparison of all Parallel Tension Data';
 proc glm data = full;
 class length width vane;
 model E = density angle length width;
 means length/TUKEY hovtest=levene;
 proc means;
 by length width vane notsorted;
run;
```

Program 2:

```
data dist;
        input angle type;
   cards;
PROC NPAR1WAY EDF;
  CLASS type;
  VAR angle;
RUN;
```

Program 3:

```
options linesize=80 pageno=1;
data normal;
input angle;
cards;
title 'Fit Weibull Distribution';
proc capability ;
      histogram /
        midpoints=5.0 to 175 by 10
        weibull;
run;
title 'Fit Normal Distribution';
proc univariate normal plot;
                  var angle;
                  histogram /
        midpoints=5.0 to 175 by 10
        normal;
run;
```

APPENDIX J: PINE SUMMARY STATISTICS

This appendix reports the material properties measured from the pine panels. The resin content, target density, press cycle, number of panel type replications and test methods are all the same as the aspen panels. Only a single strand geometry, 20 x 1.9 cm, was used for both the Lodgepole and ponderosa pine species. Tensile and compressive σ_{ult} and E were measured for both the transverse and parallel directions, as was internal bond strength. Tensile strength was calculated assuming failure within the gauge length and can be interpreted only as a limiting value (**Table A.15**). Variability is illustrated through **Table A.16**.

Specie	Parallel (MPa)				Transverse (MPa)				Internal Bond (MPa)
	Tension		Compression		Tension		Compression		
	E	σ_{ult}	E	σ_{ult}	E	σ_{ult}	E	σ_{ult}	
ponderosa	10032	33.3	7441	28.7	791	3.9	775	6.87	0.772834
Lodgepole	10677	35.9	7909	29.6	657	3.6	1072	8.55	0.698515

Table A.15: *Properties of pine panels*

Specie	Parallel % COV				Transverse % COV			
	Tension		Compression		Tension		Compression	
	E	σ_{ult}	E	σ_{ult}	E	σ_{ult}	E	σ_{ult}
ponderosa	23.7	14.6	12.6	14.4	34.1	22.7	29.7	17.1
Lodgepole	9.4	12.6	21.5	15.7	45.3	26.4	38.4	18.7

Table A.16: *Percent Coefficients of variation of pine properties*

APPENDIX K: STRAND PROPERTIES

Appendix and testing provided by Vikram Yadama.

Twenty-five aspen strands were selected to evaluate their elastic properties, E_1, E_2, G_{12}, and ν_{12} respectively. Selected strands were trimmed to square all edges and obtain clear specimen. They were conditioned at relative humidity and temperature of 55% and 75°F to achieve average equilibrium moisture content of 8% to 9%. After they were conditioned, all specimens were weighed and measured for their dimensions. Specimen length varied from approximately 4 inches to 8.5 inches. Their width ranged between 0.5-inch and 1.0-inch, and thickness varied between 0.02 inches and 0.04 inches. Strands were tested in tension without any reduction in cross-section.

Specimens were tested with tabletop Instron (Model 4466) with a 2000-lb. capacity load cell. The test specimens were loaded in tension parallel to the grain at a displacement rate of 0.01 in/min. Strands were gripped with 1-inch wide rough surface steel grips. Each strand was tested twice to measure strain in the two principal directions (longitudinal and transverse). Strain was measured at mid-length of each specimen with a 0.5-inch gage length extensometer (Model 3442-0050-020-ST, Epsilon Technology Corp.). Special extensometer grips were built to install it on the specimen to measure transverse strain. Each specimen was first instrumented to measure transverse strain, ε_x, and loaded within the elastic region to approximately to 30 pounds (approximately 25 to 40 % strand ultimate stress). Strand y-axis corresponds to the longitudinal direction and x-axis corresponds to the transverse direction. After testing all strands to measure transverse strain, they were instrumented to measure longitudinal strain, ε_y, and tested till an initial failure was detected. Specimens were weighed again and oven dried at 100 °C to determine their moisture contents and densities.

Using the measured longitudinal strain, ε_y, the modulus of elasticity, E_y, for each strand was calculated on the basis of Hooke's law. Then for each specimen, for a longitudinal stress increment of 500 psi, strain in x- and y-directions were determined and Poisson's ratio, ν_{yx}, was calculated using the relationship $-(\varepsilon_x/\varepsilon_y)$. In order to determine the elastic properties in the principal directions, it is necessary to determine the fiber orientation angle of the specimens. Fracture technique was employed to determine the fiber angle.

Fracture along the longitudinal axis at two to three locations across the specimen width was initiated to determine fiber angle in each of the specimen. Since strain was measured at mid-length of each specimen, fiber angle was measured within the half-inch gage length area where extensometer was installed. A digital picture of the area with induced fracture along the length was taken and with the aid of image analysis software, the fiber angle was estimated. Largest fiber angle recorded for each specimen was assumed to be the angle that most influences the elastic behavior of the corresponding specimen. Specimens whose fiber angle was approximately 1 degree were assumed to have orthotropic symmetry in the plane and the average of their measured modulus of elasticity and Poisson's ratio values were taken to represent E_1 and ν_{12}. Remaining strands were grouped based on their fiber angle and their average E_y and ν_{yx} values were computed.

Using the computed average values of E_1, ν_{12}, E_y, ν_{yx} and θ, tensor transformation relations were simultaneously solved to determine transverse modulus of elasticity, E_2, and shear modulus, G_{12}, for each fiber angle category.

$$\frac{1}{E_y} = \frac{1}{E_1}\cos^4\theta + \left(\frac{1}{G_{12}} - \frac{2\upsilon_{12}}{E_1}\right)\sin^2\theta\cos^2\theta + \frac{\sin^4\theta}{E_2}$$

$$\upsilon_{yx} = \frac{\upsilon_{12}(\sin^4\theta + \cos^4\theta) - (1 + \frac{E_1}{E_2} - \frac{E_1}{G_{12}})\sin^2\theta\cos^2\theta}{\cos^4\theta + (\frac{E_1}{G_{12}} - 2\upsilon_{12})\sin^2\theta\cos^2\theta + \frac{E_1}{E_2}\sin^2\theta}$$

Then, E_2 and G_{12} of all fiber angle groups were averaged to represent the corresponding E_2 and G_{12} of the strands.